PTPN2 regulates the interferon signaling and endoplasmic reticulum stress response in pancreatic β-cells in autoimmune diabetes

Bernat Elvira[1,*], Valerie Vandenbempt[1,*], Julia Bauzá-Martinez[2,3], Raphaël Crutzen[4], Javier Negueruela[1], Hazem Ibrahim[5], Matthew L. Winder[5], Manoja K. Brahma[1], Beata Vekeriotaite[1], Pieter-Jan Martens[6], Sumeet Pal Singh[7], Fernando Rossello[8], Pascale Lybaert[4], Timo Otonkoski[5], Conny Gysemans[6,#], Wei Wu[2,3,#], Esteban N. Gurzov[1]

[1]Signal Transduction and Metabolism Laboratory, Laboratoire de Gastroentérologie Expérimental et Endotools, Université libre de Bruxelles (ULB), Brussels, Belgium.
[2]Biomolecular Mass Spectrometry and Proteomics, Bijvoet Center for Biomolecular Research and Utrecht Institute for Pharmaceutical Sciences, Utrecht University, Padualaan 8, 3584 CH Utrecht, The Netherlands.
Netherlands Proteomics Centre, Padualaan 8, 3584 CH Utrecht, The Netherlands.
[4]Laboratory of Physiology and Pharmacology, Faculty of Medicine, Université Libre de Bruxelles (ULB), B-1070 Brussels, Belgium.
[5]Stem Cells and Metabolism Research Program, Faculty of Medicine, University of Helsinki, Finland.
[6]Clinical and Experimental Endocrinology (CEE), Department of Chronic Diseases, Metabolism and Ageing, Campus Gasthuisberg O&N 1, Katholieke Universiteit Leuven (KU Leuven), Leuven, Belgium.
[7]IRIBHM, Université Libre de Bruxelles (ULB), Brussels, Belgium.
[8]University of Melbourne Centre for Cancer Research University of Melbourne Melbourne Victoria Australia.

Address correspondence and reprint requests to:

Dr Esteban N. Gurzov
Signal Transduction and Metabolism Laboratory
Route de Lennik 808
Brussels, B1070
Phone: +32 2 555 8908
Email: esteban.gurzov@ulb.be

Running Title: PTPN2 modulates β-cell inflammation in type 1 diabetes

ABSTRACT

Type 1 diabetes (T1D) results from autoimmune destruction of β-cells in the pancreas. Protein tyrosine phosphatases (PTPs) are candidate genes for T1D and play a key role in autoimmune disease development and β-cell dysfunction. Here, we assessed the global protein and individual PTP profiles in the pancreas from early onset non-obese diabetic (NOD) mice treated with an anti-CD3 monoclonal antibody and interleukin-1 receptor antagonist. The treatment reversed hyperglycemia and we observed enhanced expression of PTPN2, a PTP family member and T1D candidate gene, and endoplasmic reticulum (ER) chaperones in the pancreatic islets. To address the functional role of PTPN2 in β-cells, we generated PTPN2-deficient human stem cell-derived β-like and EndoC-βH1 cells. Mechanistically, we demonstrated that PTPN2 inactivation in β-cells exacerbates type I and type II interferon signaling networks and the potential progression towards autoimmunity. Moreover, we established the capacity of PTPN2 to positively modulate the Ca^{2+}-dependent unfolded protein response and ER stress outcome in β-cells. Adenovirus-induced overexpression of PTPN2 partially protected from ER-stress induced β-cell death. Our results postulate PTPN2 as a key protective factor in β-cells during inflammation and ER stress in autoimmune diabetes.

INTRODUCTION

Type 1 diabetes (T1D) results from the progressive destruction of insulin-producing β-cells in the pancreatic islets of Langerhans mediated by local infiltration of autoimmune cells, defined as insulitis (1). During early insulitis, inflammation contributes to both the primary induction and secondary amplification of the immune assault resulting in a progressive loss of β-cells (2). The autoimmune process is quite variable between patients and within a particular subject over time (1). The progression of T1D is a non-linear process, with active and inactive autoimmunity periods in the pancreas, which can last many years. Interestingly, T-cell autoimmunity is negligible in some T1D patients (2). Islet-specific $CD8^+$ T-cells constitute a large fraction of the pancreatic $CD8^+$ T-cell population also in non-diabetic subjects (3), and it has been shown that the majority of $CD8^+$ T-cells in the T1D pancreas are not islet-specific (4). The relevance of the T-cell specificity versus non-specificity in the pancreas is unclear, but it is postulated that the dysfunction and priming of insulin-producing β-cells can occur via the release of pro-inflammatory cytokines. Thus, both type I and type II interferon (IFN) signaling are critical for the inflammatory state in invading immune cells and the target β-cells (5; 6). Cytokines released during insulitis induce dysfunction in the β-cells and trigger endoplasmic reticulum (ER) stress, contributing to β-cell death (7-9). In addition, ER stress can enhance the induction of post-translational modifications in islets (10), leading to an increase in deamidation and citrullination of islet-autoantigens, which improves the potency to bind human leukocyte antigen (HLA) molecules and their immunogenic properties.

Protein tyrosine phosphatases (PTPs) are a large superfamily of enzymes that are responsible for the modulation of cellular signaling through dephosphorylation of various tyrosine residues on intracellular proteins (11). All classical PTPs share the same catalytic mechanism with a cysteine residue essential for catalysis, located at the base of the active site (11). The Protein Tyrosine Phosphatase non-receptor 2 (*PTPN2)* gene encodes PTPN2 (also known as TC-PTP). Genome-wide association studies have identified *PTPN2* as a non-major histocompatibility complex (non-MHC) risk gene for autoimmunity, and linked 'loss of function' single nucleotide polymorphisms of PTPN2 with an increased risk of T1D development (12-14). *PTPN2* variants that affect mRNA stability or alter protein structure have also been associated with early-onset T1D (15). Interestingly, the architecture and low thiol pKa of the invariant active site cysteine in the Cys-X_5-Arg motif of PTPN2 renders the protein highly susceptible to oxidation and inactivation by reactive oxygen species, inhibiting the phosphatase activity (11). We have shown that irreversible PTPN2 oxidation occurs in the pancreas from non-obese diabetic (NOD) autoimmune mice (16). Global inactivation of PTPs by oxidative stress enhances IFN signaling in pancreatic islets leading to an increase of pro-inflammatory chemokine production and exacerbation of STAT1-induced β-cell death (16; 17). PTPN2 isoforms are generated by alternative splicing differing in the C-terminus: a 45kDa spliced variant contains a nuclear localization sequence and shuttles between the nucleus and the cytoplasm, and a 48kDa isoform is anchored to the ER (18). Several substrates have been identified for PTPN2 in different cells, including JAK1 and JAK3, Src-family, the insulin receptor, and STATs (1, 3, 5, and 6). However, the different isoforms and downstream targets by which PTPN2 modulates signaling in β-cells and autoimmune diabetes, remain poorly understood.

In the present study, we provide evidence that PTPN2 and ER chaperone expression is increased in the islets of a mouse model of reversed autoimmune diabetes. We report that PTPN2 downregulates the hyperactivation of type I and type II IFN signal transduction and participates in the unfolded protein response in β-cells. Our results shed light on mechanisms that underpin the role of PTPN2 in β-cells in T1D.

RESEARCH DESIGN AND METHODS

Mice

NOD mice, originally obtained from Dr C.Y. Wu (Peking Union Medical College Hospital, Beijing, People's Republic of China), were housed and inbred in the animal facility of Katholieke Universiteit Leuven (Leuven, Belgium) since 1989. The housing of all mice occurred under semi-barrier conditions, and animals were fed sterile food and water *ad libitum*. Mice were screened for the onset of diabetes by evaluating glucose levels in urine (Diastix Reagent Strips; Bayer, Leverkusen, Germany) and venous blood (AccuCheck; Roche Diagnostics, Vilvoorde, Belgium). Mice were diagnosed as diabetic when they had glucosuria and two consecutive blood glucose measurements exceeding 200mg/dl. Animals were maintained in accordance with the National Institutes of Health *Guide for the Care and Use of Laboratory Animals*, and all experimental procedures were approved and performed following the Ethics Committees of the Katholieke Universiteit Leuven and by the Commission d'Ethique du Bien-être Animal of the ULB (reference 732N).

Treatment was initiated on the day of the second high blood glucose measurement, designated as day 0. Hamster anti-mouse CD3 monoclonal antibody (mAb, clone145–

2C11; BioXCell, West Lebanon, NH) was administered to newly-diagnosed diabetic mice at a dose of 2.5μg/mouse intraperitoneal (i.p.) daily for 5 days (19). IL-1RA (Anakinra; Amgen, Thousand Oaks, CA) was administered at a dose of 10mg/mouse i.p. daily for 5 days. The mice were randomly assigned to treatment groups. Blood glucose values were measured twice weekly, and mice were considered in disease reversal if blood glucose measurements were <200mg/dl. Pancreases were retrieved 33 days after initiation of the therapy. However, when mice did not have disease reversal, they were culled based on human endpoints: both having dramatic weight loss over a period of less than one week and persistent hyperglycemia with values >600 mg/dl.

Cell culture and treatments

Human pancreata were obtained, with informed consent from next-of-kin, heart-beating, brain-dead donors. Human islets (kindly provided by Prof Piero Marchetti, University of Pisa, Italy, clinical characteristics available in **Supplementary Table S1**) were isolated in accordance with the local Ethical Committee in Pisa, Italy. After arrival in Brussels, islets were dispersed and cultured as previously described (20). The study was approved by the Erasme Hospital Ethics Committee.

Human Embryonic Stem Cell (hESC) H1 (WiCell, Madison, WI), and the human induced pluripotent cell (hiPSC) line Hel46.11, derived from human neonatal foreskin fibroblasts and reprogrammed using Sendai virus technology as described (21; 22), were used in the study. Undifferentiated hiPSC and hESC cells were cultured on Matrigel (Corning BV, Amsterdam, the Netherlands)-coated plates in E8 medium (Life Technologies, Carlsbad, CA). The cells were differentiated into β-like cells using a 30-

day protocol as previously described (23-25) with further modifications (**Supplementary Table S2**).

The human β-cell line EndoC-βH1 (26) (kindly provided by INNODIA consortium and Dr R. Scharfmann, University of Paris, France) was cultured in Matrigel-fibronectin-coated plates.

C57BL/6 mouse islets were washed with cell dissociation medium and dispersed into single cells by gentle continuous pipetting in trypsin (1mg/ml; Sigma-Aldrich, St Louis, MI) and DNase I (1mg/ml; Sigma-Aldrich) in a water bath at 31ºC (27). β-cell and non-β-cells were purified from dispersed islets by autofluorescence using FACS sorting (BD FACSAria™ III) and lysed with RIPA buffer for immunoblotting.

Cytokine and chemical ER stressor concentrations were selected based on previous time course and dose-response studies ((17; 28; 29), data not shown). Briefly, cells were cultured with human IFN-γ (1000U/ml, PeproTech, London, UK), IFN-α (2000U/ml, PBL Assay Science, Piscataway, NJ), IL-1β (50U/ml, R&D Systems, Minneapolis, MN), IL-10 (50ng/ml, R&D Systems), IL-6 (50U/ml, R&D Systems), IL-17 (1000ng/ml, BioLegend, San Diego, CA), IL-21 (1000ng/ml, BioLegend), IL-23 (1000ng/ml, BioLegend) or TGF-β (1000ng/ml, BioLegend). ER stress was induced by adding the SERCA blockers thapsigargin (1μM, Sigma-Aldrich), cyclopiazonic acid (CPA, 75μM, Sigma-Aldrich), tunicamycin (5μg/ml, Sigma-Aldrich), or brefeldin A (0.05μg/ml, Sigma-Aldrich) in medium containing 2% FBS. Vehicle DMSO was added to the control condition in all experiments.

Genome editing of hESCs

To knockout (KO) the *PTPN2* gene in H1 hESCs a pair of CRISPR/Cpf1 (Cas12a) gRNAs were used to remove the identified critical exon 3 which is conserved across annotated protein-coding transcripts. The 23bp gRNA sequences used to remove exon 3 (PAM: TTTA 5'-GGATTTGTCTCAACTCTATTATG-3'; and PAM: TTTC 5'-TGACGATGTAATGAATTATGGAC-3') were designed using Benchling (Biology Software, 2019). The ribonucleoprotein (RNP) components (Alt-R® A.s. Cas12a (Cpf1) Ultra and Alt-R® A.s. Cas12a crRNA) were purchased from Integrated DNA Technologies (IDT, Coralville, IA) and prepared according to the manufacturer protocol. Cells were electroporated with the RNP complexes, and single-cell clones were isolated using limiting dilution. Derived clones were screened by PCR (Primers: Fw 5'-TGGGCTTTTTCTCCTGGTGT-3'; and Rv 5'-GACGACCAGACACCATCCAG-3'), and a ~400bp deletion of exon 3 in homozygous and heterozygous KO clones was confirmed by Sanger sequencing. Generated clones were karyotyped and characterized for pluripotency using immunocytochemistry and qPCR.

Mass spectrometry, immunoprecipitation and Western blotting

For mass spectrometry analyses, specimens of frozen pancreas were disrupted by beads beating in equal weight of acid-washed glass beads, for 10min at 4^{o}C (30s on/off cycles). To prevent experimentally induced oxidation, lysis buffer (10% glycerol, 1% NP-40, 1x complete EDTA-free protease inhibitor cocktail (Roche Diagnostics, Basel, Switzerland), 1x phosphatase inhibitor (Sigma-Aldrich)) was degassed with Helium for 20min before use. After tissue disruption, lysed samples were further sonicated for 10min at 4^{o}C (30s on/off cycles), and insoluble debris was pelleted at 20,000g for 1h at

4°C. The supernatant was retained for subsequent analysis of total PTP. Chemical derivatization was performed with 10mM DTT for 1h. Subsequently hyperoxidation was performed with 1mM pervanadate, for 30min in the dark. The derivatized tissue lysates were then reduced in 4mM DTT for 1h at 20°C and alkylated in 8mM iodoacetamide for 30min at 20°C in the dark, for subsequent digestion with Lys C (1:50) (Fujifilm Wako, Neuss, Germany) for 4h at 37°C, and then Trypsin (1:50) (Sigma-Aldrich) for 16h at 37°C. Digested tryptic peptides were diluted in PBS for oxPTP pulldown. Per sample, 10µl of Protein A/G agarose beads (Santa Cruz, Dallas, TX) were coated with 10µg of oxPTP antibody (R&D Systems) for immuno-retrieval of oxPTP peptides. Eluted peptides were cleaned up with home-made Strong Cation Exchange (SCX) micro STAGE tips. LC-MS/MS analyses of resulting oxPTP peptides were performed as described previously (30). 2µg PTPN2 antibody was used for immunoprecipitation, 50µl of Protein A/G agarose beads (Thermofisher, Waltham, MA) were used for immuno-retrieval of PTPN2-binding proteins.

For western blotting, cells were lysed using RIPA buffer, total proteins were extracted and resolved by 12% SDS-PAGE, transferred onto a nitrocellulose membrane and immunoblotted with antibodies described in **Supplementary Table S3** (31). The intensity values of the protein bands were corrected by the values of the housekeeping protein GAPDH, β-actin or α-tubulin used as loading controls.

RNA interference, adenoviral transduction and cell viability

EndoC-βH1 and dispersed human islets have been transfected with small interfering RNAs (siRNAs) or allstars Negative control siRNA (30nM, Qiagen, Venlo, the Netherlands) using Lipofectamine RNAiMAX (Invitrogen, Carlsbad, CA) as

previously described (20). siRNA target sequences are provided in **Supplementary Table S4**.

Adenoviruses carrying green fluorescent protein (GFP) as reporter, a cytomegalovirus promoter and PTPN2 gene or scrambled control were developed by Sirion Biotech (Martinsried, Germany). Virus amplification, purification, titration, and verification were done by Sirion Biotech.

The percentage of viable and apoptotic cells was determined either by inverted fluorescence microscopy with the DNA dyes Hoechst 342 (20µg/ml) and propidium iodide (10µg/ml) (9; 32) or by flow cytometry with Zombie Aqua™ Fixable Viability Kit (1:500, Biolegend) and measured with a BD FACSCanto™ II Cell Analyzer (BD Bioscience, San Jose, CA). Viability by fluorescence microscopy was evaluated by at least two independent observers with one of them unaware of sample identity.

Real-time PCR and RNA sequencing (RNA-Seq)

Poly(A)+ mRNA extraction was performed using Dynabeads mRNA DIRECT kit (Invitrogen) following the manufacturer's instructions; reverse transcription was carried out using a reverse transcriptase kit (Eurogentec, Seraing, Belgium). Quantitative real-time PCR was performed using Bio-Rad CFX machine (Bio-Rad, Hercules, CA) and the SYBR Green reagent (Bio-Rad). β-actin and/or GAPDH were used as internal controls. Probe and primer details are provided in **Supplementary Table S5**.

The total RNA was obtained using QIAamp® DNA mini kit (Qiagen, Hilden, Germany) following the manufacturer's instructions. RNA quality analysis, library

preparation and sequencing were performed by the BRIGHT core facility (Brussels, Belgium). The sequencing was performed on an Illumina Novaseq 600. An average of 25 million paired-end reads of 100 nucleotides long were obtained per sample. The list of up/downregulated genes/transcripts and association with canonical pathways were determined using the online degust software with Limma/Voom and packages EGSEA and ComplexHeatmap in RStudio (Boston, MA). The modulated transcription factors were analyzed by the online software Predicting ASsociated Transcription factors from Annotated Affinities (PASTAA) using the default settings (33). To perform the Rank-Rank Hypergeometric test, the RRHO and RRHO2 packages were used in RStudio.

Intracellular calcium concentration measurements and patch-clamp

EndoC-βH1 cells were transfected with siRNA for 72h followed by incubation with fura-2 acetoxymethyl ester (1μM) for 1h at 37°C in Krebs solution (115mM NaCl, 5mM KCl, 1mM $CaCl_2$, 1mM $MgCl_2$, 24mM $NaHCO_3$, 0.20% BSA and 10mM HEPES with pH adjusted to 7.4) supplemented with 0.5mM glucose. The coverslips were then transferred to a tissue chamber filled with Krebs solution supplemented with 1mM glucose and mounted on an inverted fluorescence microscope (Diaphot TDM; Nikon, Tokyo, Japan) for epifluorescence. Fura-2 fluorescence of single cells was measured by dual-excitation fluorimetry using a camera-based image analysis system (Magical; Applied Imaging, Sunderland, UK). The excitation and emission wavelengths were set at 340/380 and 510nm, respectively, and pair images (at the excitations of 340 and 380nm, 30ms interval) were taken every 2.5s. Intracellular Ca^{2+} concentration was calculated from the ratios of the 340 and 380nm signals as previously described using Metafluor software (Molecular Devices, San Jose, CA) (9; 34).

Patch-clamp of differentiated H1 PTPN2 KO and control aggregates were conducted as previously described (35). For voltage measurements, gramicidin-perforated whole-cell configuration patch-clamp experiments were conducted. Bath solution contained: 110mM NaCl, 10mM HEPES, 4mM KCl, 1mM $MgCl_2$, 1mM $CaCl_2$, 24mM $NaHCO_3$; pH 7.4 with NaOH supplemented with 2.8 or 20mM D-glucose, osmolarity 299 or 319mOsmol/l. Pipette solution contained: 10mM NaCl, 20mM KCl, 24mM K_2SO_4, 90mM KCl, 25.9mM D-mannitol, 5mM HEPES; pH 7.2 with KOH, supplemented with 50 to 150ng/ml gramicidin, osmolarity 304mOsmol/l. Stock solution of gramicidin (5mg/ml in DMSO) was daily prepared. Filled pipettes had resistances of 8-10MΩ. Whole-cell configuration induced by gramicidin permeabilization was achieved within 15 to 20 min. Leak resistance after sealing above 1.5GΩ and access resistance (Rs)<35MΩ were required to allow the recordings. Aggregates were stored in an incubator and used within 1h incubation in the patch-clamp chamber. Voltages were monitored with a HEKA EPC-10 amplifier (HEKA Elektronik GmbH, Lamprecht, Germany). Zero current whole-cell voltages were continuously recorded using PatchMaster software (HEKA Elektronik GmbH, Lamprecht, Germany).

Immunofluorescence

Cells were fixed using 4% PFA (Sigma-Aldrich), permeabilized with 0.5% Triton X-100 (Sigma-Aldrich) and unspecific binding sites blocked using Ultravision protein block (Thermofisher). Cells were then incubated with primary antibodies overnight at 4°C followed by 1h incubation with the secondary antibody conjugated to the fluorochrome (**Supplementary Table S3**). Next, cells were mounted using

Vectashield® antifade medium mounting with 4′,6-diamidino-2-phenylindole (DAPI, Sigma-Aldrich).

Mouse pancreata were fixed with formalin and embedded in paraffin. Sections (5-10µm) were dewaxed, and antigen unmasking was performed using heated sodium citrate buffer. Sections were permeabilized using 0.1% Triton X-100 and unspecific binding sites were blocked using 5% normal goat or donkey serum (Sigma-Aldrich) according to the host of the secondary antibody for 1h at RT. After blocking, sections were incubated with primary antibodies as described in **Supplementary Table S3**, then incubated with Alexa-fluor® (Thermofisher) secondary antibodies except for BiP/GRP78 Alexa fluor 488 and counterstained with DAPI (1µg/mL, Sigma-Aldrich).

Images were analyzed on AxioImager Z1 microscope using Zeiss Zen blue software (Carl Zeiss AG, Germany). The fluorescence intensity quantification within the murine pancreas section was analyzed using CellProfiler software (Broad Institute, Cambridge, MA).

Statistical analysis

The results are presented as the mean ± standard error of the mean (SEM). Student's t-test was used for comparisons between two groups. Differences among groups were assessed by two-way ANOVA or repeated-measures ANOVA. Statistical analyses were assessed using Prism software (GraphPad Software 8, Inc, La Jolla, CA). Sample size was predetermined based on the variability observed in prior experiments and on preliminary data. Differences were regarded as statistically significant if *$p< 0.05$; **$p< 0.01$; ***$p< 0.001$.

Data and Resource Availability

The RNA-Seq dataset generated during the sequencing procedure is deposited in the Gene Expression Omnibus database (access number GSE172148), the mass spectrometry proteomics and peptidomics data have been deposited to the ProteomeXchange Consortium via the PRIDE (access number PXD025394) and available from the corresponding author upon reasonable request.

RESULTS

Proteomic screening identifies increased pancreatic chaperones and PTPN2 expression in NOD mice with diabetes remission after anti-CD3 + IL-1RA treatment.

To identify anti-inflammatory targets in NOD mice with reversed hyperglycemia, we took advantage of non-Fc receptor (FcR) binding anti-CD3 mAb and IL-1RA treatment to preserve insulin production (36) and assessed protein expression and PTP profile in the pancreas. We confirmed that administration of anti-CD3 + IL-1RA in a small cohort of hyperglycemic mice significantly reversed diabetes, compared with a low dose of anti-CD3 alone used as control (not cured, **Figure 1A**). We isolated snap-frozen pancreas from treated NOD mice and performed a mass spectrometry analysis, as previously described (30; 31). Samples were divided to detect the global protein profile, PTP spectral counts and individual PTPs (**Supplementary Figure S1A**). We detected 1452 proteins, from those 117 upregulated and 8 downregulated proteins were significantly modulated in the anti-CD3 + IL-1RA group compared to the controls (**Figure 1B**). Pathway analysis showed that ER stress response and protein folding are at the top of the significantly modulated pathways in the cured mice (**Figure 1C**). We observed increased expression of the chaperones BiP, GRP94, Hsph1, Erp44, and

chaperone/associated protein MANF (**Figure 1D**). In addition, we observed protein modulation of eukaryotic initiator factors and the oxidative stress response in the pancreas from anti-CD3 + IL-1RA treated mice (**Supplementary Figure S1B**). Anti-CD3 + IL-1RA therapy impacts pro-inflammatory cytokine signaling (36). To identify tyrosine phosphatase expression, all PTPs were reduced in the sample by treatment with dithiothreitol (DTT), followed by hyperoxidation using pervanadate, which converts all catalytic cysteines of PTPs into the sulphonic acid (SO_3H) state, allowing detection of phosphatases by immunoprecipitation with an ox-PTP antibody binding to the majority of classical PTPs (**Supplementary Figure S1A**). Out of 17 PTP motif peptides detected (**Supplementary Figure S1C**), 2 were found significantly regulated in NOD mice with reversed diabetes, namely PTPN2 was increased and PTPN13 decreased compared to controls (**Figure 1E**). PTPN2 is a candidate gene for T1D development and PTPN13 (Fap-1) is a negative regulator of apoptotic cell death induced by Fas (37). PTPN2 is expressed in FACS-purified β-, non-β-, and acinar cells from C57BL/6 mice (**Figure 1F**). Interestingly, NOD islets showed lower levels of PTPN2 compared to C57BL/6 islets (**Figure 1G**). We observed a low expression of PTPN2 in immune infiltrated islets from non-cured control, anti-CD3 or anti-IL-1RA treated mice (**Figure 1H, Supplementary Figures S2 and S3**). Conversely, PTPN2 is highly expressed in insulin-positive cells, and also detected in surrounding immune cells (insulitis) in the anti-CD3 + IL-1RA treated mice (**Figure 1H, Supplementary Figures S2 and S3**). Moreover, PTPN2, BiP, GRP94 and MANF positively correlated with insulin in the islets (**Figure 1H and I, Supplementary Figures S4, S5 and S6).** IL-1β treatment did not affect PTPN2 expression in mouse islets, EndoC-βH1 cells, or β-like cells (**Supplementary Figure S7A-C**). It was previously shown that the combination

therapy induced immune regulatory mechanisms (36), including increased Foxp3^{+} splenic Tregs and IL-10 production. We observed that IL-10 + IFN-γ (induced by anti-CD3) significantly upregulated PTPN2 expression in EndoC-βH1cells (**Figure 1J**). We concluded that members of the unfolded protein response and PTPN2 expression in β-cells/islets positively correlates with β-cell survival in the anti-CD3 + IL-1RA treated NOD mice.

PTPN2 modulates the IFN-γ-mediated inflammatory response through STAT1 phosphorylation in human β-like and EndoC-βH1 cells.

To gain mechanistic insight into the role of PTPN2 in pancreatic β-cells, we first took advantage of a well-established 7-stage differentiation protocol to evaluate the expression of PTPN2 in differentiated β-like cells. OCT4, SOX17, PDX1, NKX6.1, glucagon, and insulin have been used as differentiation markers (**Figure 2A, Supplementary Figure S8A**). We achieved an average of 30-40% efficiency of insulin-positive cells (**Figure 2B, Supplementary Figure S8B**). Interestingly, PTPN2 protein expression was significantly decreased from stage 4 in the β-like cell differentiation of both Hel46.11 and H1 stem cells (**Figure 2C** and data not shown). We knocked out PTPN2 using CRISPR/Cpf1 deletion of exon 3 in H1 cells (**Figure 2D, Supplementary Figure S9A-D**). Both PTPN2 knockout and control H1 hESC were differentiated into insulin-producing β-like cells (**Supplementary Figure S9E**). To mimic the β-cell response to a localized autoimmune attack, we pulsed differentiated β-like cells with 1h exposure of IFN-γ followed by a washout of the cytokine and subsequent analysis of activated signaling at different time points (chase). We first focused on STAT1, an IFN-induced transcription factor that has been implicated in β-cell dysfunction and death (17; 38). PTPN2 deletion by

CRISPR/Cpf1 prolonged the chase activation of STAT1 by phosphorylation after a 1h pulse of IFN-γ in β-like cells (**Figure 2E**).

Stem cell differentiation produces a mix of hormone expressing endocrine-like cells. To study PTPN2-modulated signaling specifically in human insulin-producing β-cells, we took advantage of EndoC-βH1cells and siRNA technology. We selected the siRNAs with higher PTPN2 knockdown efficiency (#3 and #4) from the 6 different siRNAs tested (**Figure 2F**). Cells were transfected with siRNA PTPN2 (number #4, unless otherwise indicated), treated with IFN-γ in a 1h pulse and chase experiment, and the effect of PTPN2 knockdown on the kinetics and magnitude of IFN-γ-induced STAT1 and STAT3 phosphorylation was evaluated. The IFN-γ mediated phosphorylation of STAT1/3 proteins occurred with different kinetics in the EndoC-βH1, but it was markedly prolonged in cells in which PTPN2 was knocked down (**Figure 2G, Supplementary Figure S10**).

Given that PTPN2 deficiency enhanced STAT activity, we next asked whether the downstream gene targets are affected. In keeping with previous studies (17; 38), we observed increased CXCL9, CXCL10 and HLA/MHC class I activation in PTPN2 knocked down cells (**Figure 2H**). Both STAT1 and STAT3 are phosphorylated on tyrosine residues, forming dimers through the reciprocal SH2 domain/phosphotyrosine interactions and binding to γ-activated sequence elements. However, STAT1 and STAT3 dimers selectively bind to similar but not identical elements (39). To assess the transcription factor responsible for chemokine expression in PTPN2-inhibited cells, we silenced PTPN2 and STAT1 or STAT3 in a double-knockdown approach (**Figure 2I**). As previously shown, inhibition of PTPN2 significantly exacerbated CXCL9 and CXCL10

expression 24h after the pulse with IFN-γ. This effect was abrogated by STAT1 but not STAT3 knockdown (**Figure 2I**), suggesting that STAT1 is the main inflammatory enhancer driving chemokine expression in IFN-γ-treated PTPN2-deficient β-cells.

Inactivation of PTPN2 increases and prolongs type I and type II IFN-signaling in β-cells.

Elevated levels of type I IFN were found exclusively in the pancreas and islets from T1D patients (6; 40) and has been associated with the early stages of the development of autoimmune diabetes in humans (41) and rodents (42). We performed a 1h IFN-α pulse and chase experiment in PTPN2-deficient β-like and EndoC-βH1 cells. Similar to IFN-γ-treated cells, PTPN2 inactivation increased STAT1 phosphorylation (**Figure 3A and B**). PTPN2-mediated STAT1 hyperactivation was markedly prolonged after the pulse of IFN-γ (**Figure 2D**) compared to IFN-α (**Figure 3A**). Similar results were observed between PTPN2-deficient β-like and EndoC-βH1 cells treated with IFN-γ or IFN-α (**Figures 2F and 3B**). Next, we performed RNA-Seq analysis of type I and type II IFN treated PTPN2-deficient and control EndoC-βH1 cells to determine the comprehensive footprint induced 24h after the 1h exposure to the different cytokines. First, we validated the PTPN2 knockdown efficiency, insulin levels and STAT1-modulated gene expression in the samples (**Figure 3C**). No differences were observed in glucose-stimulated insulin secretion after PTPN2 knockdown in EndoC-βH1 cells (**Supplementary Figure S11**). As expected, STAT1-targets SOCS1, CXCL9, CXCL10 and CXCL11 were upregulated in PTPN2-deficient IFN-γ-treated EndoC-βH1 cells (**Figure 3C**). Profiling of the dataset using the Gene Ontology (GO) method for gene set testing allowed us to identify several modulated pathways by PTPN2

silencing including the unfolded protein response (**Figure 3D**). To refine the potential list of PTPN2 target genes, we analyzed the top upregulated and downregulated genes and pathways affected by control and type I and type II IFN treated cells (**Figure 3E, Supplementary Figures S12 and S13**). Knockdown of PTPN2 upregulated T1D-related pathways: antigen processing and presentation via MHC class I, antigen processing and presentation of peptide antigen, and response to IFN (**Supplementary Figure S12**). In addition, PTPN2 deficiency significantly increased the persistent activation of gene expression induced by the pro-inflammatory cytokines (**Figure 3F and G**).

To identify transcription factors responsible for gene network modulation by PTPN2, we used the PASTAA software (33) (**Figure 4A**). The signature of transcription factors SP1, STAT, IRF and NF-κB responsible for immune signaling in β-cells (29; 43) was increased after PTPN2 knockdown and IFN-γ treatment. We observed enhanced degradation of IκBα, a repressor of NF-κB, in IFN-γ-treated PTPN2 knockdown cells (**Figure 4B**). NF-Y, associated with MHC gene expression (44), was found to be at the top of the PTPN2-modulated transcription factor in IFN-α-treated cells (**Figure 4A**). We performed a Rank-Rank Hypergeometric Overlap (RRHO) analysis (45), comparing ranked lists of genes identified by RNA-Seq of primary β-cells of individuals affected by T1D (46) and our dataset. There is a low or no correlation between EndoC-βH1 siRNA control cells 24h after the 1h pulse with either IFN-γ or IFN-α and the data set of T1D β-cells (**Figure 4C**). In contrast, we observed an overlap between gene profiles of PTPN2-deficient EndoC-βH1 cells exposed to IFN-γ or IFN-α and β-cells from T1D individuals (**Figure 4C**). In addition, PTPN2 deficiency in β-cells enhanced activation of additional cytokines involved in autoimmunity, i.e., IL-6,

IL-21, IL-23 and TGF-β (**Figure 4D-F**) (47). Overall, our results demonstrate a critical anti-inflammatory role of PTPN2 in the control of cytokine signaling in β-cells.

PTPN2 deficiency sensitizes β-cells to Ca^{2+}-dependent Endoplasmic Reticulum stress

We observed increased PTPN2 and ER chaperone proteins in anti-CD3 + IL-1RA-treated NOD mice (**Figure 1**) and modulation of unfolded protein response genes/ER stress by IFN-γ in PTPN2-deficient β-cells (**Figure 3G**). A 48kDa ER-located isoform of PTPN2 has been previously identified (18), but its role in β-cells in autoimmune diabetes remains unknown. To determine if PTPN2 regulates the unfolded protein response activation, we tested different chemical ER stressors. Interestingly, PTPN2 deficiency increased β-cell death induced by Ca^{2+}-dependent ER stress (thapsigargin and CPA) but did not impact tunicamycin toxicity induced by inhibition of the N-glycosylation in protein folding (**Figure 5A, Supplementary Figure S14A**). In line with these observations, PTPN2-deficient β-cells have reduced Ca^{2+} levels in the ER (**Figure 5B**). The effect of PTPN2 inactivation in dysregulated Ca^{2+} homeostasis was not due to major changes in mRNA expression levels of the Ca^{2+} channels inositol triphosphate (IP_3), ryanodine receptor 2, the sarco/endoplasmic reticulum Ca^{2+}-ATPase (SERCA)-2 pump or the voltage-gated Ca^{2+} (CaV) channels (**Supplementary Figure S14B**). We detected BiP in the pulldown of EndoC-βH1 overexpressing PTPN2, suggesting a direct protein-protein interaction (**Supplementary Figure S14C**). PTPN2 knockdown enhanced mRNA and protein expression of ER stress markers in thapsigargin treated EndoC-βH1 cells (**Figure 5C and D**). Prolonged activation of the PERK/eIF2α/ATF4/Chop pathway results in cell death. Importantly, we confirmed our results in PTPN2 knockout β-like cells and dispersed human islet cells transfected with

PTPN2 siRNAs. Thus, thapsigargin increased ER stress-associated pathways in PTPN2-deficient cells (**Figure 5E and F, Supplementary Figure 14D**).

Ca^{2+} homeostasis is directly linked to membrane potential and β-cell function. Zero-current gramicidin-perforated patch-clamp voltage recordings were performed on insulin-producing H1 PTPN2 KO and control aggregates stimulated with 20 mM glucose (**Figure 6A**). H1 control cells displayed a limited electrical activity at 2.8 mM glucose and it is increased after 20 mM glucose stimulation, which approximates a normal β-cell response. Interestingly, the PTPN2 KO cells from aggregates constantly displayed a strong electrical activity at the different glucose concentrations (**Figure 6A**), suggesting a dysregulated hyperactivation of the voltage-dependent Ca^{2+} and Na^{+} channels.

Next, we examined whether overexpression of different PTPN2 isoforms protects β-cells from dysregulated Ca^{2+}-induced ER stress and cell death. The 45kDa or the 48kDa PTPN2 isoforms were overexpressed using adenoviral vectors containing the human PTPN2 cDNA under the control of the cytomegalovirus promoter. PTPN2 protein levels were efficiently increased in EndoC-βH1 at the different MOIs tested (**Figure 6B, Supplementary Figure S15A**). We selected MOI 50 for subsequent experiments showing increased PTPN2 expression (**Figure 6B and C**) and low toxicity (**Supplementary Figure S15B**). The 45kDa PTPN2 isoform abrogated IFN-γ-induced STAT1 phosphorylation (**Supplementary Figure S15C**) but did not impact on Ca^{2+}-dependent ER stress-induced cells death (**Supplementary Figure S15D**). The 48kDa PTPN2 isoform decreased thapsigargin-and CPA-mediated cell death (**Figure 6D and E**) but did not affect Ca^{2+}-independent ER stress toxicity induced by tunicamycin or

brefeldin A (**Supplementary Figure S15E**). Importantly, EndoC-βH1 cells transduced with 48 kDa AdPTPN2 decreased thapsigargin-induced caspase-3 activation and BiP protein expression (**Figure 6F and G**). Taken together, our data show an isoform dependent PTPN2 modulation of IFN-induced gene signaling and ER stress-mediated apoptosis in β-cells.

DISCUSSION

The ability to modulate selectively inflammatory signal transduction pathways holds therapeutic potential for T1D and other autoimmune disorders (48). In the present study, we established the capacity of PTPN2 to prevent inflammatory signaling and to positively modulate the Ca^{2+}-dependent unfolded protein response in pancreatic β-cells. In particular, we demonstrated that PTPN2 deficiency exacerbates both type I and type II IFN dependent networks in β-cells, and the potential progression towards autoimmunity. In addition, our study suggests that the localized activity of PTPN2, in concert with other protective pathways (7; 8; 29; 49), can ameliorate the development of ER stress in β-cells.

The JAK/STAT signaling pathway induces immune-mediated β-cell dysfunction and death in T1D (5). We observed that PTPN2 deficiency in the β-cells resulted in increased STAT1 activation and downstream targets of type I and type II IFNs, in line with previous studies (17; 38). We went beyond and provided a comprehensive gene network regulated by PTPN2 contributing to the amplification of the inflammatory response. There is a strong correlation between the levels of STAT1 measured in the β-cells of patients with T1D and HLA-I hyperexpression, and the IFN gene signature (50). STAT1 deficiency in NOD mice prevents islet inflammation (51) and protects β-

cells against immune-mediated destruction induced by multiple low doses of streptozotocin (52). Our results have demonstrated that PTPN2 deficiency exacerbates STAT1 and other transcription factor activity, affecting approximately double of the IFN-modulated gene inflammatory signature of β-cells. It is conceivable that β-cells with deficient PTPN2 activity are more susceptible to the autoimmune attack in T1D. In keeping with this, we demonstrated an association between gene expression induced by PTPN2 deficiency and IFN treatment in EndoC-βH1cells and β-cells from T1D individuals (46). Moreover, PTPN2 deficiency in β-cells also enhances STAT1/3 activation of IL-6, IL-21, IL-23 and TGF-β, pro-inflammatory cytokines involved in autoimmune diabetes (47).

It has been long known that insulin-producing β-cells have a developed ER and are consequently more prone to ER stress than non-secretory cells (9; 53). This susceptibility has been postulated as one of the initial mechanisms of β-cell dysfunction and death in early T1D (7; 54). Thus, ER stress triggers β-cell dysfunction and apoptosis during inflammation (8; 53). The unfolded protein response aims to alleviate ER stress by induction of transcription of genes linked to protein folding. We observed upregulation of BiP, GRP94, MANF and PTPN2 in the pancreas/islets from anti-CD3 + IL-1RA-treated NOD mice. This eventually allows β-cells to maintain functionality and survive the autoimmune storm (49). PTPN2 have been previously associated with ER stress regulation and β-cell function in obesity (55; 56). We demonstrated that PTPN2 regulates the Ca^{2+}-dependent pathway of the unfolded protein response. PTPN2 deficiency affected inactivation of the SERCA pump leading to ER Ca^{2+} depletion (CPA and thapsigargin) but did not impact on inhibition of N-linked protein glycosylation in the ER (tunicamycin) or inhibition of vesicle formation and transport

between the ER and the Golgi apparatus (brefeldin A), suggesting specificity of PTPN2 activity at the ER. High levels of ER Ca^{2+} are required to promote proper protein folding (57), as ER resident chaperones have Ca^{2+}-dependent regulatory motifs. We postulate that PTPN2 deficiency induces Ca^{2+} leak at the ER sensitizing β-cells to hyperactivation of the PERK/eIF2α/ATF4/Chop pathway. BiP is a major ER chaperone protein and has a role in binding Ca^{2+} to buffer around 25% of the luminal Ca^{2+} load (57). PTPN2 regulates and directly binds to BiP in β-cells (present data). BiP expression was upregulated by PTPN2 deficiency and attenuated by PTPN2 overexpression in β-cells exposed to SERCA blockers. Interestingly, BiP post-translational modifications are associated with antigen presentation and the autoimmune process (58).

PTPN2 expression in the pancreas correlated positively with anti-CD3 + IL-1RA therapy outcome in a small cohort of NOD mice. We did not observe diabetes remission in anti-CD3 treated mice. This is probably due to the low concentration of anti-CD3 mAb and the number of mice used in our study. It is expected that in large cohorts, a percentage of mice can be cured with the mono-therapies (19), and PTP/protein expression should be analyzed in the different sub-groups. In addition, measurements of PTPN2/chaperone mRNA and protein expression at different time points in large cohorts of β-cell-specific PTPN2 knockout/wild type NOD mice will be required to gain additional *in vivo* mechanistically insight. This is beyond the scope of the present work. Although in this study we focused our attention on the role of PTPN2 in the β-cells and islets, it is conceivable that PTPN2 in immune cells also contributes to the amelioration of the inflammatory process of autoimmune diabetes. Consistent with this, $CD8^+$ T-cells lacking PTPN2 and cross-primed by β-cell self-antigens escape tolerance

and acquire cytotoxic T-cell activity, resulting in β-cell destruction in the RIP-mOVA mouse model of autoimmune diabetes (59). Moreover, T-cell PTPN2 deficiency in NOD mice accelerated the onset and increased the incidence of diabetes (60). Additional work is required to determine if overexpression of PTPN2 in immune cells and/or β-cells can prevent or reverse the development of autoimmune diabetes in patients. Importantly, we have demonstrated that our proteomic approach can be integrated in future studies to determine protein expression and PTP levels in pancreatic cells in T1D samples.

In conclusion, we demonstrated that PTPN2 inactivation plays a key anti-inflammatory role in β-cell dysfunction in the context of IFN signaling and ER stress. PTPN2 deficiency can light up the "danger signal" in early T1D and, together with the local amplification of pro-inflammatory cytokines and chemokines, activate the expansion of the autoimmune cells. Our findings provide fundamental evidence that PTPN2 is an important regulator of β-cell inflammation and support the active role of β-cells in their own demise in T1D.

ACKNOWLEDGMENTS

We thank Madalina Popa, André Dias, Grégory Vegh, personnel from the ULB Center for Diabetes Research (Université libre de Bruxelles) and Marijke Viaene (Katholieke Universiteit Leuven) for experimental and technical support, Alessandra K. Cardozo (Université libre de Bruxelles) for critical reading of the manuscript, and Piero Marchetti and the Pancreatic Islet Laboratory in Pisa (University of Pisa) for human islets. The authors declare no conflict of interest.

FUNDING

This work was supported by a Fonds National de la Recherche Scientifique (FNRS)-MIS grant (33650793), a European Research Council (ERC) Consolidator grant METAPTPs (GA817940), a JDRF Career Development Award (CDA-2019-758-A-N). BE and VV are supported by a FNRS CR postdoctoral fellowship (34769436) and PhD Aspirant scholarship, respectively. SPS is supported by MISU funding from the FNRS (34772792 – SCHISM). ENG is a Research Associate of the FNRS, Belgium.

AUTHOR CONTRIBUTIONS

BE, VV, JBM, RC, JN, HI, MLW, MKB, BV and PJM research data and reviewed and edited the manuscript. SPS and FR contributed to data analysis. PL, TO, CG, WW contributed to research data, experimental design and reviewed and edited the manuscript. ENG research data; contributed to designed experiments; and reviewed, edited, and wrote the manuscript. ENG is the guarantor of this work and, as such, had full access to all the data in the study and take responsibility for the integrity of the data and the accuracy of the data analysis.

REFERENCES

1. Christoffersson G, Rodriguez-Calvo T, von Herrath M. Recent advances in understanding Type 1 Diabetes. F1000Res 2016;5
2. Claessens LA, Wesselius J, van Lummel M, Laban S, Mulder F, Mul D, Nikolic T, Aanstoot HJ, Koeleman BPC, Roep BO. Clinical and genetic correlates of islet-autoimmune signatures in juvenile-onset type 1 diabetes. Diabetologia 2020;63:351-361
3. Bender C, Rodriguez-Calvo T, Amirian N, Coppieters KT, von Herrath MG. The healthy exocrine pancreas contains preproinsulin-specific CD8 T cells that attack islets in type 1 diabetes. Sci Adv 2020;6

4. Roep BO, Thomaidou S, van Tienhoven R, Zaldumbide A. Type 1 diabetes mellitus as a disease of the beta-cell (do not blame the immune system?). Nat Rev Endocrinol 2020;
5. Gurzov EN, Stanley WJ, Pappas EG, Thomas HE, Gough DJ. The JAK/STAT pathway in obesity and diabetes. FEBS J 2016;283:3002-3015
6. Huang X, Yuang J, Goddard A, Foulis A, James RF, Lernmark A, Pujol-Borrell R, Rabinovitch A, Somoza N, Stewart TA. Interferon expression in the pancreases of patients with type I diabetes. Diabetes 1995;44:658-664
7. Clark AL, Urano F. Endoplasmic reticulum stress in beta cells and autoimmune diabetes. Curr Opin Immunol 2016;43:60-66
8. Gurzov EN, Eizirik DL. Bcl-2 proteins in diabetes: mitochondrial pathways of beta-cell death and dysfunction. Trends Cell Biol 2011;21:424-431
9. Cardozo AK, Ortis F, Storling J, Feng YM, Rasschaert J, Tonnesen M, Van Eylen F, Mandrup-Poulsen T, Herchuelz A, Eizirik DL. Cytokines downregulate the sarcoendoplasmic reticulum pump Ca2+ ATPase 2b and deplete endoplasmic reticulum Ca2+, leading to induction of endoplasmic reticulum stress in pancreatic beta-cells. Diabetes 2005;54:452-461
10. Thomaidou S, Zaldumbide A, Roep BO. Islet stress, degradation and autoimmunity. Diabetes Obes Metab 2018;20 Suppl 2:88-94
11. Gurzov EN, Stanley WJ, Brodnicki TC, Thomas HE. Protein tyrosine phosphatases: molecular switches in metabolism and diabetes. Trends Endocrinol Metab 2015;26:30-39
12. Barrett JC, Clayton DG, Concannon P, Akolkar B, Cooper JD, Erlich HA, Julier C, Morahan G, Nerup J, Nierras C, Plagnol V, Pociot F, Schuilenburg H, Smyth DJ, Stevens H, Todd JA, Walker NM, Rich SS, Type 1 Diabetes Genetics C. Genome-wide association study and meta-analysis find that over 40 loci affect risk of type 1 diabetes. Nat Genet 2009;41:703-707
13. Espino-Paisan L, de la Calle H, Fernandez-Arquero M, Figueredo MA, de la Concha EG, Urcelay E, Santiago JL. A polymorphism in PTPN2 gene is associated with an earlier onset of type 1 diabetes. Immunogenetics 2011;63:255-258
14. Bieschke J, Herbst M, Wiglenda T, Friedrich RP, Boeddrich A, Schiele F, Kleckers D, Lopez del Amo JM, Gruning BA, Wang Q, Schmidt MR, Lurz R, Anwyl R, Schnoegl S, Fandrich M, Frank RF, Reif B, Gunther S, Walsh DM, Wanker EE. Small-molecule conversion of toxic oligomers to nontoxic beta-sheet-rich amyloid fibrils. Nat Chem Biol 2011;8:93-101
15. Okuno M, Ayabe T, Yokota I, Musha I, Shiga K, Kikuchi T, Kikuchi N, Ohtake A, Nakamura A, Nakabayashi K, Okamura K, Momozawa Y, Kubo M, Suzuki J, Urakami T, Kawamura T, Amemiya S, Ogata T, Sugihara S, Fukami M, Japanese Study Group of Insulin Therapy for C, Adolescent D. Protein-altering variants of PTPN2 in childhood-onset Type 1A diabetes. Diabet Med 2018;35:376-380
16. Stanley WJ, Litwak SA, Quah HS, Tan SM, Kay TW, Tiganis T, de Haan JB, Thomas HE, Gurzov EN. Inactivation of Protein Tyrosine Phosphatases Enhances Interferon Signaling in Pancreatic Islets. Diabetes 2015;64:2489-2496
17. Santin I, Moore F, Colli ML, Gurzov EN, Marselli L, Marchetti P, Eizirik DL. PTPN2, a candidate gene for type 1 diabetes, modulates pancreatic beta-cell apoptosis via regulation of the BH3-only protein Bim. Diabetes 2011;60:3279-3288

18. ten Hoeve J, de Jesus Ibarra-Sanchez M, Fu Y, Zhu W, Tremblay M, David M, Shuai K. Identification of a nuclear Stat1 protein tyrosine phosphatase. Mol Cell Biol 2002;22:5662-5668
19. Takiishi T, Korf H, Van Belle TL, Robert S, Grieco FA, Caluwaerts S, Galleri L, Spagnuolo I, Steidler L, Van Huynegem K, Demetter P, Wasserfall C, Atkinson MA, Dotta F, Rottiers P, Gysemans C, Mathieu C. Reversal of autoimmune diabetes by restoration of antigen-specific tolerance using genetically modified Lactococcus lactis in mice. J Clin Invest 2012;122:1717-1725
20. Gurzov EN, Barthson J, Marhfour I, Ortis F, Naamane N, Igoillo-Esteve M, Gysemans C, Mathieu C, Kitajima S, Marchetti P, Orntoft TF, Bakiri L, Wagner EF, Eizirik DL. Pancreatic beta-cells activate a JunB/ATF3-dependent survival pathway during inflammation. Oncogene 2012;31:1723-1732
21. Trokovic R, Weltner J, Noisa P, Raivio T, Otonkoski T. Combined negative effect of donor age and time in culture on the reprogramming efficiency into induced pluripotent stem cells. Stem Cell Res 2015;15:254-262
22. Achuta VS, Grym H, Putkonen N, Louhivuori V, Karkkainen V, Koistinaho J, Roybon L, Castren ML. Metabotropic glutamate receptor 5 responses dictate differentiation of neural progenitors to NMDA-responsive cells in fragile X syndrome. Dev Neurobiol 2017;77:438-453
23. Saarimaki-Vire J, Balboa D, Russell MA, Saarikettu J, Kinnunen M, Keskitalo S, Malhi A, Valensisi C, Andrus C, Eurola S, Grym H, Ustinov J, Wartiovaara K, Hawkins RD, Silvennoinen O, Varjosalo M, Morgan NG, Otonkoski T. An Activating STAT3 Mutation Causes Neonatal Diabetes through Premature Induction of Pancreatic Differentiation. Cell Rep 2017;19:281-294
24. Pagliuca FW, Millman JR, Gurtler M, Segel M, Van Dervort A, Ryu JH, Peterson QP, Greiner D, Melton DA. Generation of functional human pancreatic beta cells in vitro. Cell 2014;159:428-439
25. Rezania A, Bruin JE, Arora P, Rubin A, Batushansky I, Asadi A, O'Dwyer S, Quiskamp N, Mojibian M, Albrecht T, Yang YH, Johnson JD, Kieffer TJ. Reversal of diabetes with insulin-producing cells derived in vitro from human pluripotent stem cells. Nat Biotechnol 2014;32:1121-1133
26. Ravassard P, Hazhouz Y, Pechberty S, Bricout-Neveu E, Armanet M, Czernichow P, Scharfmann R. A genetically engineered human pancreatic beta cell line exhibiting glucose-inducible insulin secretion. J Clin Invest 2011;121:3589-3597
27. Schaschkow A, Pang L, Vandenbempt V, Elvira B, Litwak SA, Vekeriotaite B, Maillard E, Vermeersch M, Paula FMM, Pinget M, Perez-Morga D, Gough DJ, Gurzov EN. STAT3 Regulates Mitochondrial Gene Expression in Pancreatic beta-Cells and Its Deficiency Induces Glucose Intolerance in Obesity. Diabetes 2021;70:2026-2041
28. Meyerovich K, Violato NM, Fukaya M, Dirix V, Pachera N, Marselli L, Marchetti P, Strasser A, Eizirik DL, Cardozo AK. MCL-1 Is a Key Antiapoptotic Protein in Human and Rodent Pancreatic beta-Cells. Diabetes 2017;66:2446-2458
29. Gurzov EN, Ortis F, Cunha DA, Gosset G, Li M, Cardozo AK, Eizirik DL. Signaling by IL-1beta+IFN-gamma and ER stress converge on DP5/Hrk activation: a novel mechanism for pancreatic beta-cell apoptosis. Cell Death Differ 2009;16:1539-1550
30. Wu W, Hale AJ, Lemeer S, den Hertog J. Differential oxidation of protein-tyrosine phosphatases during zebrafish caudal fin regeneration. Sci Rep 2017;7:8460

31. Gurzov EN, Tran M, Fernandez-Rojo MA, Merry TL, Zhang X, Xu Y, Fukushima A, Waters MJ, Watt MJ, Andrikopoulos S, Neel BG, Tiganis T. Hepatic oxidative stress promotes insulin-STAT-5 signaling and obesity by inactivating protein tyrosine phosphatase N2. Cell Metab 2014;20:85-102
32. Litwak SA, Wali JA, Pappas EG, Saadi H, Stanley WJ, Varanasi LC, Kay TW, Thomas HE, Gurzov EN. Lipotoxic Stress Induces Pancreatic beta-Cell Apoptosis through Modulation of Bcl-2 Proteins by the Ubiquitin-Proteasome System. J Diabetes Res 2015;2015:280615
33. Roider HG, Manke T, O'Keeffe S, Vingron M, Haas SA. PASTAA: identifying transcription factors associated with sets of co-regulated genes. Bioinformatics 2009;25:435-442
34. Van Eylen F, Lebeau C, Albuquerque-Silva J, Herchuelz A. Contribution of Na/Ca exchange to Ca2+ outflow and entry in the rat pancreatic beta-cell: studies with antisense oligonucleotides. Diabetes 1998;47:1873-1880
35. Crutzen R, Virreira M, Markadieu N, Shlyonsky V, Sener A, Malaisse WJ, Beauwens R, Boom A, Golstein PE. Anoctamin 1 (Ano1) is required for glucose-induced membrane potential oscillations and insulin secretion by murine beta-cells. Pflugers Arch 2016;468:573-591
36. Ablamunits V, Henegariu O, Hansen JB, Opare-Addo L, Preston-Hurlburt P, Santamaria P, Mandrup-Poulsen T, Herold KC. Synergistic reversal of type 1 diabetes in NOD mice with anti-CD3 and interleukin-1 blockade: evidence of improved immune regulation. Diabetes 2012;61:145-154
37. Gump JM, Staskiewicz L, Morgan MJ, Bamberg A, Riches DW, Thorburn A. Autophagy variation within a cell population determines cell fate through selective degradation of Fap-1. Nat Cell Biol 2014;16:47-54
38. Moore F, Colli ML, Cnop M, Esteve MI, Cardozo AK, Cunha DA, Bugliani M, Marchetti P, Eizirik DL. PTPN2, a candidate gene for type 1 diabetes, modulates interferon-gamma-induced pancreatic beta-cell apoptosis. Diabetes 2009;58:1283-1291
39. Qing Y, Stark GR. Alternative activation of STAT1 and STAT3 in response to interferon-gamma. J Biol Chem 2004;279:41679-41685
40. Foulis AK, Farquharson MA, Meager A. Immunoreactive alpha-interferon in insulin-secreting beta cells in type 1 diabetes mellitus. Lancet 1987;2:1423-1427
41. Ferreira RC, Guo H, Coulson RM, Smyth DJ, Pekalski ML, Burren OS, Cutler AJ, Doecke JD, Flint S, McKinney EF, Lyons PA, Smith KG, Achenbach P, Beyerlein A, Dunger DB, Clayton DG, Wicker LS, Todd JA, Bonifacio E, Wallace C, Ziegler AG. A type I interferon transcriptional signature precedes autoimmunity in children genetically at risk for type 1 diabetes. Diabetes 2014;63:2538-2550
42. Carrero JA, Benshoff ND, Nalley K, Unanue ER. Type I and II Interferon Receptors Differentially Regulate Type 1 Diabetes Susceptibility in Male Versus Female NOD Mice. Diabetes 2018;67:1830-1835
43. Moore F, Naamane N, Colli ML, Bouckenooghe T, Ortis F, Gurzov EN, Igoillo-Esteve M, Mathieu C, Bontempi G, Thykjaer T, Orntoft TF, Eizirik DL. STAT1 is a master regulator of pancreatic {beta}-cell apoptosis and islet inflammation. J Biol Chem 2011;286:929-941
44. Sachini N, Papamatheakis J. NF-Y and the immune response: Dissecting the complex regulation of MHC genes. Biochim Biophys Acta Gene Regul Mech 2017;1860:537-542

45. Plaisier SB, Taschereau R, Wong JA, Graeber TG. Rank-rank hypergeometric overlap: identification of statistically significant overlap between gene-expression signatures. Nucleic Acids Res 2010;38:e169
46. Russell MA, Redick SD, Blodgett DM, Richardson SJ, Leete P, Krogvold L, Dahl-Jorgensen K, Bottino R, Brissova M, Spaeth JM, Babon JAB, Haliyur R, Powers AC, Yang C, Kent SC, Derr AG, Kucukural A, Garber MG, Morgan NG, Harlan DM. HLA Class II Antigen Processing and Presentation Pathway Components Demonstrated by Transcriptome and Protein Analyses of Islet beta-Cells From Donors With Type 1 Diabetes. Diabetes 2019;68:988-1001
47. Clark M, Kroger CJ, Tisch RM. Type 1 Diabetes: A Chronic Anti-Self-Inflammatory Response. Front Immunol 2017;8:1898
48. Gurzov EN, Ke PC, Ahlgren U, Garcia Ribeiro RS, Gotthardt M. Novel Strategies to Protect and Visualize Pancreatic beta Cells in Diabetes. Trends Endocrinol Metab 2020;31:905-917
49. Engin F, Yermalovich A, Nguyen T, Hummasti S, Fu W, Eizirik DL, Mathis D, Hotamisligil GS. Restoration of the unfolded protein response in pancreatic beta cells protects mice against type 1 diabetes. Sci Transl Med 2013;5:211ra156
50. Richardson SJ, Rodriguez-Calvo T, Gerling IC, Mathews CE, Kaddis JS, Russell MA, Zeissler M, Leete P, Krogvold L, Dahl-Jorgensen K, von Herrath M, Pugliese A, Atkinson MA, Morgan NG. Islet cell hyperexpression of HLA class I antigens: a defining feature in type 1 diabetes. Diabetologia 2016;59:2448-2458
51. Kim S, Kim HS, Chung KW, Oh SH, Yun JW, Im SH, Lee MK, Kim KW, Lee MS. Essential role for signal transducer and activator of transcription-1 in pancreatic beta-cell death and autoimmune type 1 diabetes of nonobese diabetic mice. Diabetes 2007;56:2561-2568
52. Gysemans CA, Ladriere L, Callewaert H, Rasschaert J, Flamez D, Levy DE, Matthys P, Eizirik DL, Mathieu C. Disruption of the gamma-interferon signaling pathway at the level of signal transducer and activator of transcription-1 prevents immune destruction of beta-cells. Diabetes 2005;54:2396-2403
53. Scheuner D, Kaufman RJ. The unfolded protein response: a pathway that links insulin demand with beta-cell failure and diabetes. Endocr Rev 2008;29:317-333
54. Tersey SA, Nishiki Y, Templin AT, Cabrera SM, Stull ND, Colvin SC, Evans-Molina C, Rickus JL, Maier B, Mirmira RG. Islet beta-cell endoplasmic reticulum stress precedes the onset of type 1 diabetes in the nonobese diabetic mouse model. Diabetes 2012;61:818-827
55. Bettaieb A, Liu S, Xi Y, Nagata N, Matsuo K, Matsuo I, Chahed S, Bakke J, Keilhack H, Tiganis T, Haj FG. Differential regulation of endoplasmic reticulum stress by protein tyrosine phosphatase 1B and T cell protein tyrosine phosphatase. J Biol Chem 2011;286:9225-9235
56. Xi Y, Liu S, Bettaieb A, Matsuo K, Matsuo I, Hosein E, Chahed S, Wiede F, Zhang S, Zhang ZY, Kulkarni RN, Tiganis T, Haj FG. Pancreatic T cell protein-tyrosine phosphatase deficiency affects beta cell function in mice. Diabetologia 2015;58:122-131
57. Preissler S, Rato C, Yan Y, Perera LA, Czako A, Ron D. Calcium depletion challenges endoplasmic reticulum proteostasis by destabilising BiP-substrate complexes. Elife 2020;9
58. Buitinga M, Callebaut A, Marques Camara Sodre F, Crevecoeur I, Blahnik-Fagan G, Yang ML, Bugliani M, Arribas-Layton D, Marre M, Cook DP, Waelkens E, Mallone

R, Piganelli JD, Marchetti P, Mamula MJ, Derua R, James EA, Mathieu C, Overbergh L. Inflammation-Induced Citrullinated Glucose-Regulated Protein 78 Elicits Immune Responses in Human Type 1 Diabetes. Diabetes 2018;67:2337-2348
59. Wiede F, Ziegler A, Zehn D, Tiganis T. PTPN2 restrains CD8 T cell responses after antigen cross-presentation for the maintenance of peripheral tolerance in mice. Journal of autoimmunity 2014;53:105-114
60. Wiede F, Brodnicki TC, Goh PK, Leong YA, Jones GW, Yu D, Baxter AG, Jones SA, Kay TWH, Tiganis T. T-Cell-Specific PTPN2 Deficiency in NOD Mice Accelerates the Development of Type 1 Diabetes and Autoimmune Comorbidities. Diabetes 2019;68:1251-1266

FIGURE LEGENDS

Figure 1. Treatment with anti-CD3 + IL-1RA reversed diabetes in newly-diagnosed diabetic NOD mice with an increase of protein levels of PTPN2 and chaperons in pancreatic islets. (A) Newly-diagnosed diabetic NOD mice were treated with anti-CD3 mAb + IL-1RA or anti-CD3 as control. Murine blood glucose was examined by glucometer two times weekly for 32 days. n=5. **(B)** Volcano plots of up (red) or down (blue) regulated proteins in the mass spectrometry analysis. n=5. **(C)** Enriched pathway analysis of combined anti-CD3 + IL-1RA treatment or anti-CD3 control pancreas. Only pathways with $p < 0.05$ are shown. **(D)** Protein profile of pancreata was examined by mass spectrometry. Protein expression of ER stress response-related proteins is shown. LFQ: label-free quantification. n=5. **(E)** Protein expression of PTPs in anti-CD3 + IL-1RA or control pancreas examined by mass spectrometry. n=3-5. (**F**) Expression of PTPN2 was determined in FACS-purified β, non-β and acinar cells. Western blot representative of 2 independent experiments. (**G**) Islets were isolated from 12-week-old C57BL/6, 6- and 12-week-old NOD mice. Gene expression of PTPN2 and β-actin was examined by qPCR. n=3-4. **(H)** Immunofluorescence analysis of insulin and BiP or PTPN2 in pancreas sections. The nuclei were visualized with DAPI. PTPN2 or BiP and insulin-positive cells are shown

(white arrows). Scale bar: 50µm. (**I**) Insulin and PTPN2 correlation in pancreatic islets from anti-CD3 + IL-1RA treatment is shown. (**J**) EndoC-βH1 cells were treated with IL-10 + IFN-γ as indicated. PTPN2 and β-actin were assessed by qPCR. n=4. *p<0.05,**p<0.01.

Figure 2. PTPN2 regulates IFN-γ signaling in pancreatic β-cells. (A) Immunofluorescence staining of Hel46.11 hiPSC differentiation markers in the different stages as indicated. Insulin positive cells are shown (white arrows). Scale bar: 50µm. **(B)** Insulin mRNA expression was assessed by real-time PCR in the different stages of Hel46.11 hiPSC differentiation into β-like cells. Results were normalized with the mean of GAPDH and β-actin as internal housekeeping genes (HKG). n=5. **(C)** Western blot for PTPN2 expression in H1 hESC differentiation into β-like cells. The relative protein expression of the PTPN2 shown was quantified by dividing the intensity values against GAPDH as internal housekeeping protein using the ImageJ® software. **(D)** Western blot for PTPN2 was performed in undifferentiated H1 hESC cells with CRISPR/Cpf1 deletion of PTPN2: H1 wild-type (+/+), H1 heterozygous knockout (+/-) and H1 homozygous knockout (-/-). Western blot is representative of 2 independent experiments. **(E)** hESC-derived β-like cells (H1 control and H1 homozygous PTPN2 knockout (H1 PTPN2 KO)) were cultured with 1h pulse of IFN-γ followed by a change of the media and starting of the chase (Ch) measures at the indicated time points. Western blot for pSTAT1, total STAT1 and PTPN2 was performed. n=4. **(F)** EndoC-βH1 cells were transfected with control or 6 different PTPN2 siRNAs. n=4. **(G)** Transfected cells with control or PTPN2 siRNA were cultured with IFN-γ for 1h in a pulse-chase experiment. Western blot for pSTAT1/3 and total STAT1/3 was performed. n=4. **(H)** Transfected cells with control or PTPN2 siRNA were cultured

with IFN-γ for 1h in a pulse-chase experiment. Gene expression was examined by qPCR. n=4-5. **(I)** Transfected cells with control or double transfection with PTPN2, STAT1 and/or STAT3 siRNA were cultured with IFN-γ for 1h. Gene expression of PTPN2, STAT1, STAT3 and chemokines was examined by qPCR, 24h after cytokine treatment. n=4. *p<0.05, **p<0.01, ***p<0.001.

Figure 3. PTPN2 is a master regulator of type I and type II IFN associated pathways in β-cells. (A) hESC-derived β-like cells were cultured with 1h pulse of the pro-inflammatory cytokine IFN-α followed by a change of the media and starting of the chase (Ch) measures at the indicated times. Western blot for pSTAT1, total STAT1 and PTPN2 was performed. Western blot representative of 3 independent experiments. **(B)** Transfected EndoC-βH1 cells with control or PTPN2 siRNA were cultured with IFN-α for 1h in a pulse-chase experiment. n=4. **(C)** Gene counts obtained by RNA-Seq were normalized to reads per kilobase million (RPKM) using RStudio. n=3. **(D)** Pathway enrichment analysis of the comparison between siRNA PTPN2 or control transfected EndoC-βH1 cells obtained by RNA-Seq. The length of the bars is proportional to the level of significant change, expressed by the negative logarithm of the adjusted p-value. Pathways are considered significantly modulated upon $-\log_{10}$(p. adj) > 1.3. **(E)** The top 10 most significant up or downregulated genes in the RNA-Seq dataset are visualized by heatmaps, the counts are scaled to the difference of the row mean. Gene expression is considered significant upon an FDR<0.05. n=3. **(F)** Volcano plots of up (red) or down (blue) regulated genes in the RNA-Seq dataset for the effect of IFN-γ, IFN-α in siRNA control or siRNA PTPN2 cells transfected EndoC-βH1 cells. Genes are considered significantly modulated upon log fold change > 1 and $-\log_{10}$(FDR) > 1.3. **(G)** The Venn diagram represents the overlap of genes modulated in the different groups. Gene

expression is considered significant upon an FDR<0.05. n=3. *p<0.05, **p<0.01, ***p<0.001.

Figure 4. Gene modulation by PTPN2 under pro-inflammatory cytokine stimulation correlates with gene expression of primary β-cells from T1D individuals. (A) Modulated transcription factors regulated by PTPN2, and pro-inflammatory cytokine stimulation were predicted using the PASTAA software. The 10 most associated transcription factors are shown ($p < 0.05$). **(B)** Transfected EndoC-βH1 cells with control or PTPN2 siRNA were cultured with IFN-γ for 1h in a pulse-chase experiment. pSTAT1, IκBα, β-actin, PTPN2 and GAPDH were determined by Western blot. n=4. **(C)** Gene counts obtained by RNA-Seq were RRHO comparison analysis was performed using RStudio. (**D**) Transfected cells with control or PTPN2 siRNA were cultured with IL-6 for 1h. Western blot for pSTAT1/3, total STAT1/3, PTPN2 and GAPDH was performed. n=4. (**E**) hESC-derived β-like cells were cultured with IL-6 for 1h. Western blot for pSTAT1/3, total STAT1/3, PTPN2 and GAPDH was performed. n=3. (**F**) Transfected EndoC-βH1 cells with control or PTPN2 siRNA were cultured with the pro-inflammatory cytokines as indicated for 1h. Western blot for pSTAT3, total STAT3, PTPN2 and GAPDH was performed. n=4. *p<0.05, **p<0.01, ***p<0.001.

Figure 5. PTPN2 modulates SERCA/Ca^{2+}-mediated cell death, ER stress marker expression and Ca^{2+} intracellular levels in β-cells. (A) Transfected EndoC-βH1 cells with control or 2 different PTPN2 siRNAs were treated with thapsigargin or CPA for 48h. β-cell apoptosis was evaluated by Hoechst 33342/propidium iodide staining. n=4-5. **(B)** Intracellular calcium levels were measured by Fura-2 dye in transfected EndoC-

βH1 cells with PTPN2 or control siRNAs. Thapsigargin was added as indicated, and the area under the curve (AUC) was measured. n=4. **(C)** Transfected EndoC-βH1 cells with PTPN2 or control siRNAs were cultured with thapsigargin for 48h. Gene expression of PTPN2 and ER stress markers was examined by qPCR. n=3-6. **(D)** Transfected EndoC-βH1 cells with PTPN2 or control siRNAs were cultured with thapsigargin for 48h. Protein expression of ER stress markers was examined by Western blot. n=3-4. **(E)** Dispersed H1-derived β-like cells were cultured with thapsigargin 24 or 48h as indicated. Protein expression of ER chaperone BiP was examined by Western blot. n=3. **(F)** Transfected dispersed human islets with PTPN2 or control siRNAs were cultured with thapsigargin for 24h. Gene expression of PTPN2 and ER stress markers was examined by qPCR. n=3. *p<0.05, **p<0.01, ***p<0.001.

Figure 6. PTPN2 deficiency affects the membrane potential, and its overexpression ameliorates SERCA/Ca^{2+}-mediated ER stress in β-cells. (A) Zero-current gramicidin-perforated patch-clamp voltage recordings. Sampling rate, 5kHz. Dotted lines represent zero-voltage level. **1-3** Glucose-stimulated in differentiated H1 control aggregates (2.8 and 20mM glucose), **4-6** Glucose-stimulated in differentiated H1 PTPN2 KO aggregates (2.8 and 20mM glucose). **1, 4** magnification of the electrical activity of the cells during min 3 with 2.8mM glucose in the bath medium. **2, 5** magnification of the electrical activity of the cells during min 10 with 20mM glucose in the bath medium. **3, 6** magnification of the electrical activity of the cells during min 25 with 2.8mM glucose in the bath medium after the 20mM glucose stimulation. Measurement representative of 2 independent experiments. **(B)** EndoC-βH1 cells were transduced with inactive adenovirus (AdControl), AdPTPN2 45kDa or AdPTPN2 48kDa. The relative protein expression of the PTPN2 was determined using Western

blot 72h after transduction. n=3. **(C)** Immunofluorescence staining of PTPN2 in EndoC-βH1 cells transduced with AdPTPN2 48kDa or AdControl. PTPN2 overexpression in AdPTPN2 48kDa is shown (white arrows). The nuclei were visualized with DAPI. Scale bar: 20µm. **(D)** Transduced cells with AdPTPN2 48kDa or AdControl were cultured with CPA for 48h. β-cell apoptosis was evaluated by Hoechst 33342/propidium iodide staining. n=3. (**E-G).** Transduced cells with AdPTPN2 48kDa or AdControl were cultured with thapsigargin for 48h. (E) β-cell apoptosis was evaluated by Hoechst 33342/propidium iodide staining. n=5. (F) Cleaved caspase-3 activation was evaluated by Western blot in cells transduced with AdPTPN2 48kDa or AdControl and treated with thapsigargin for 48h as indicated. n=2. (G) Transduced cells with AdPTPN2 48kDa or AdControl were cultured with thapsigargin for 48h. Expression of ER stress marker BiP was examined by Western blot. n=5. *p<0.05, **p<0.01, ***p<0.001.

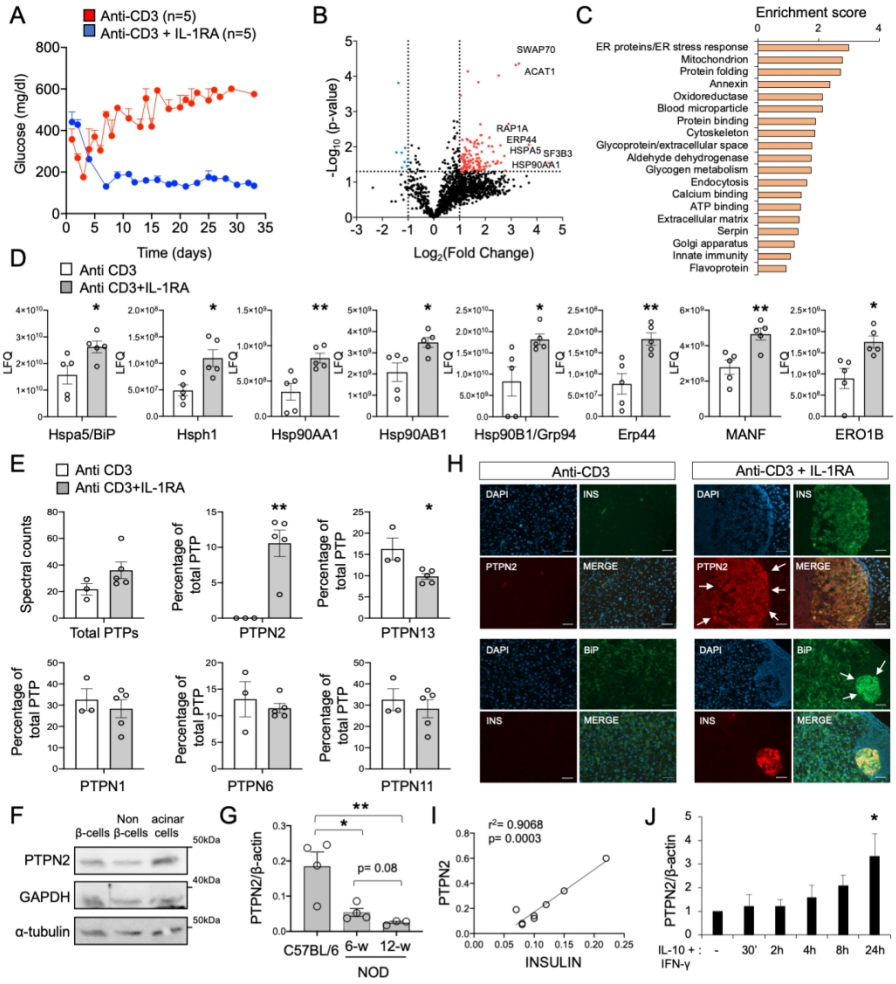

Figure 1

266x355mm (137 x 137 DPI)

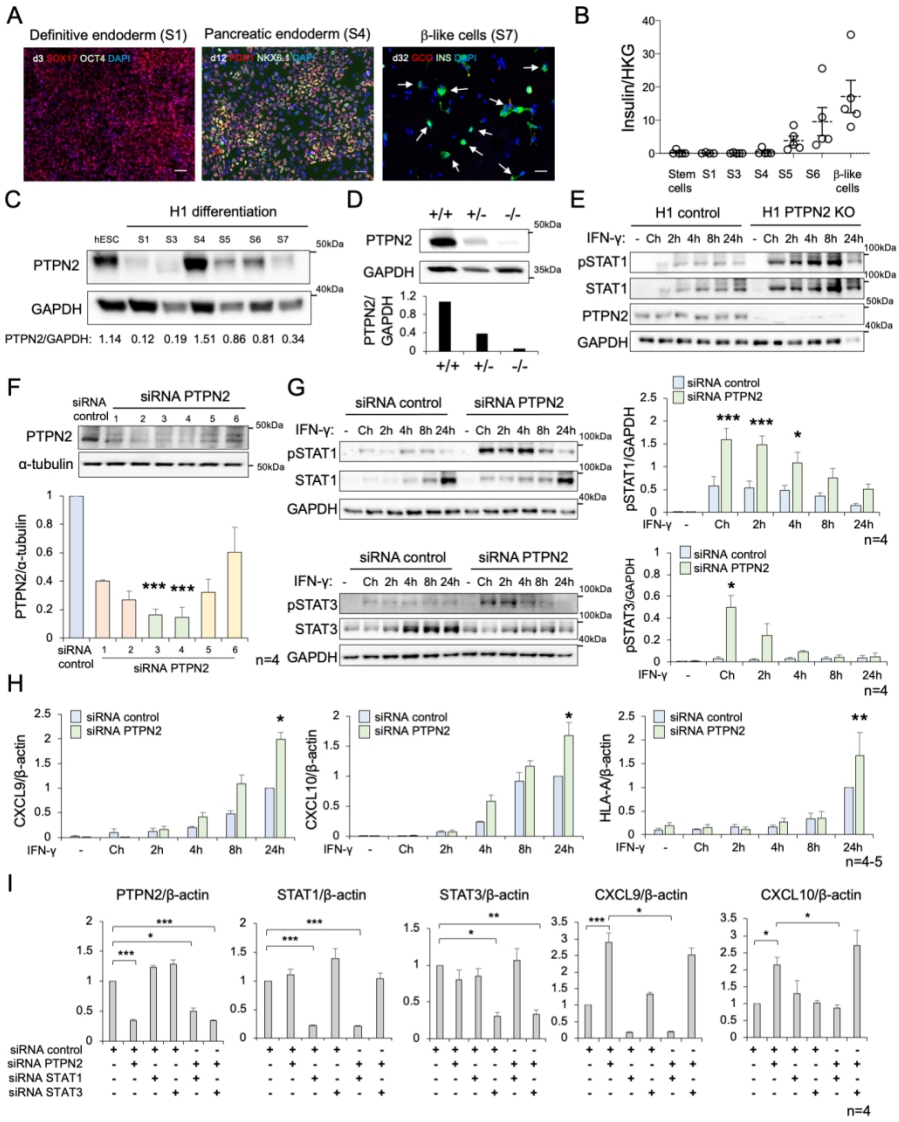

Figure 2

266x355mm (137 x 137 DPI)

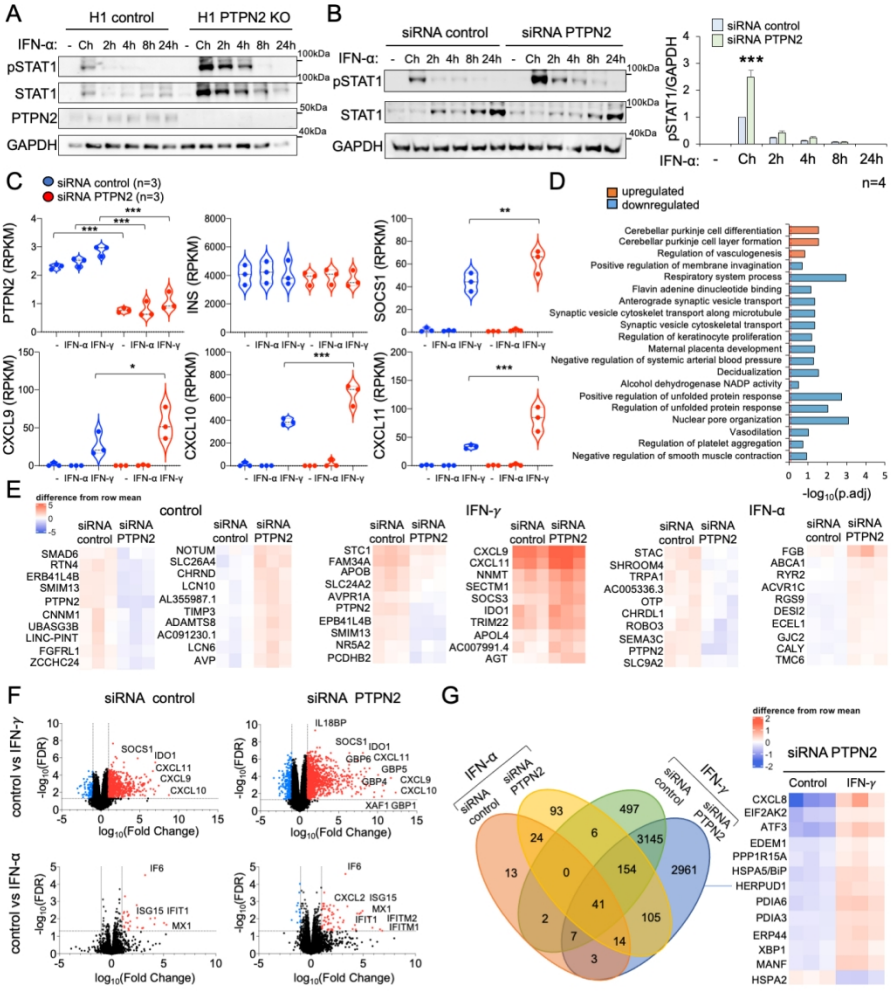

Figure 3

266x355mm (137 x 137 DPI)

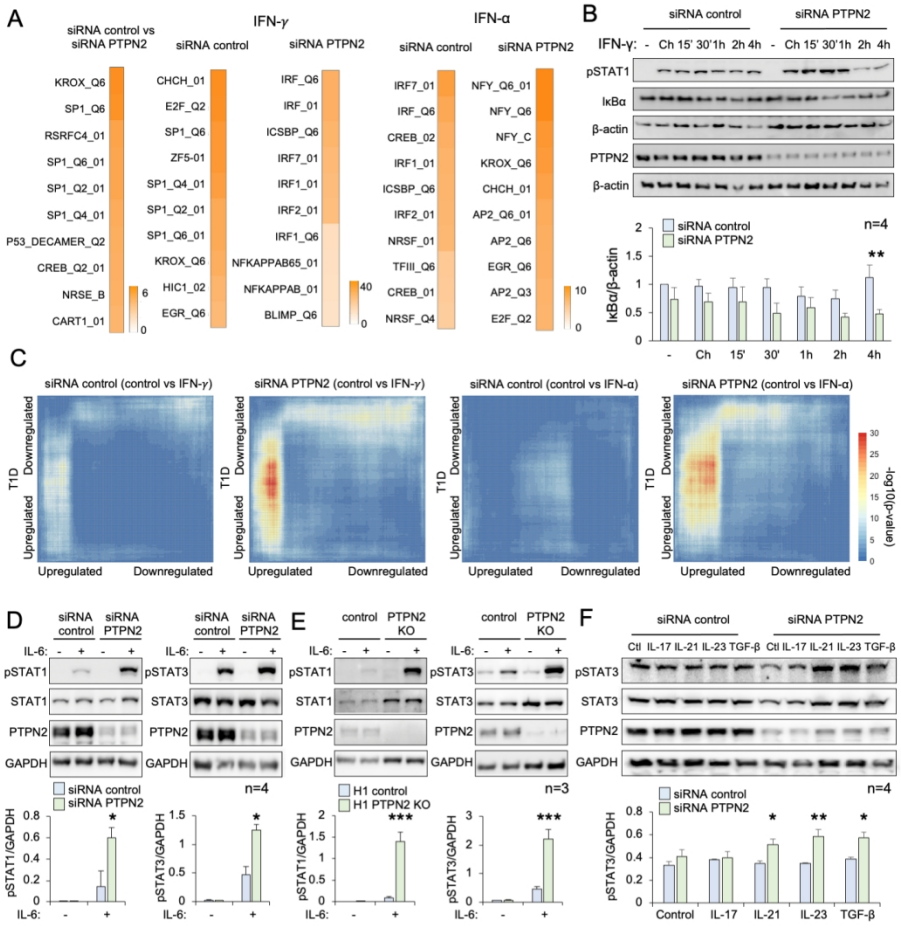

Figure 4

266x355mm (137 x 137 DPI)

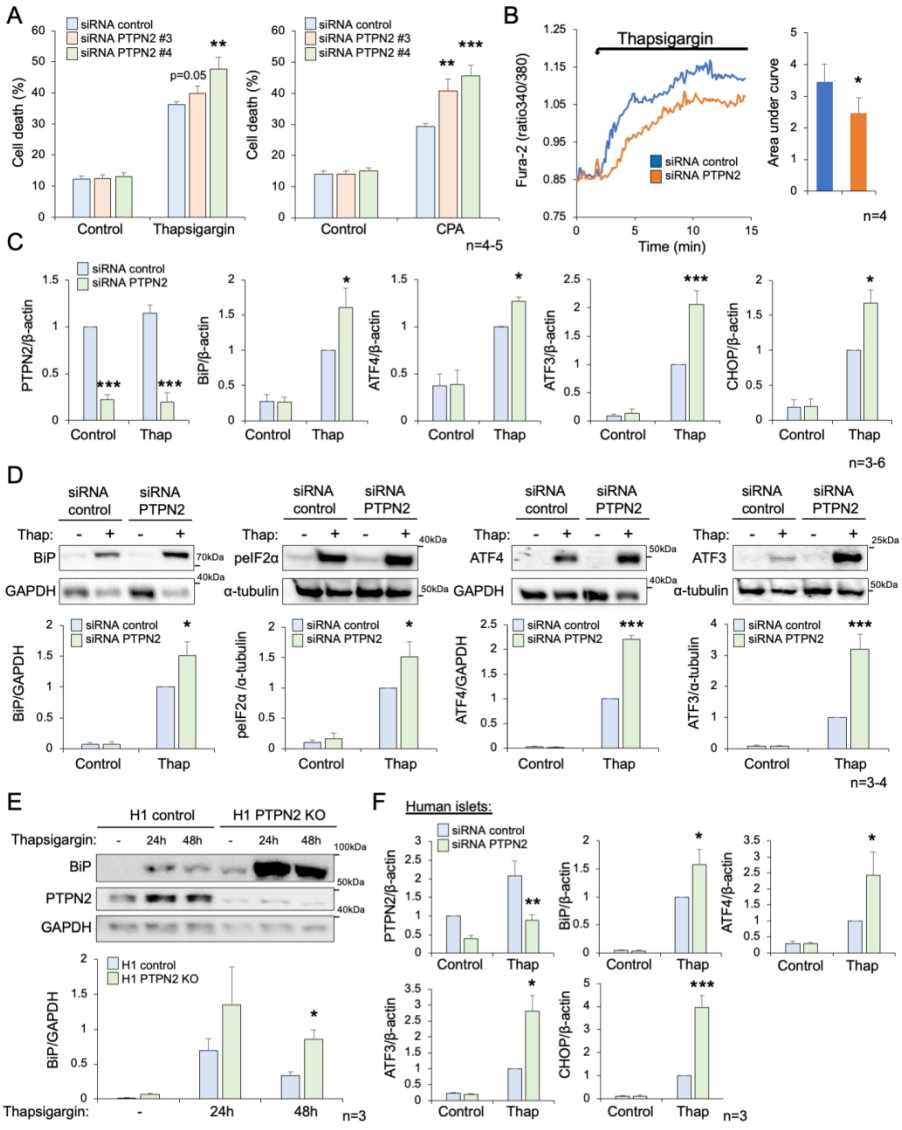

Figure 5

266x355mm (137 x 137 DPI)

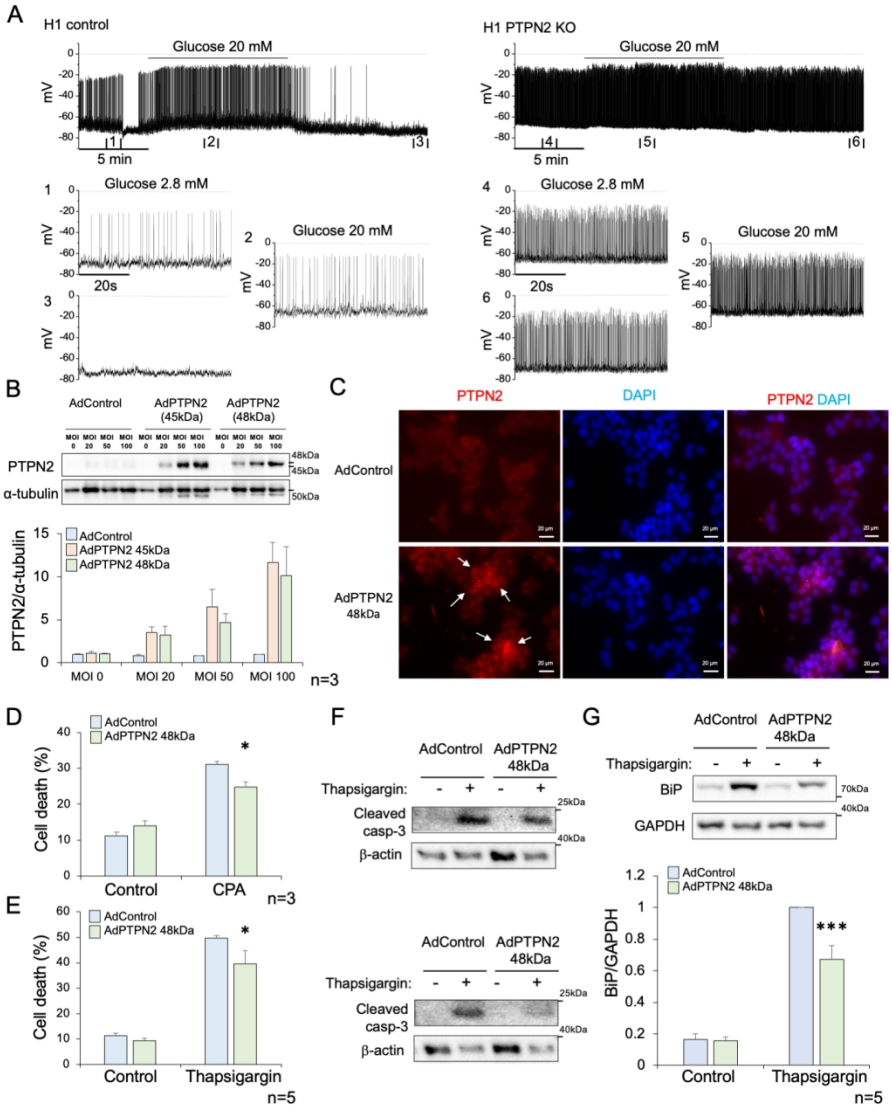

Figure 6

266x355mm (137 x 137 DPI)

Supplemental Data.

PTPN2 regulates the interferon signalling and endoplasmic reticulum stress response in pancreatic β-cells in autoimmune diabetes

Bernat Elvira, Valerie Vandenbempt, Julia Bauzá-Martinez, Raphaël Crutzen, Javier Negueruela, Hazem Ibrahim, Matthew L. Winder, Manoja K. Brahma, Beata Vekeriotaite, Pieter-Jan Martens, Sumeet Pal Singh, Fernando Rossello, Pascale Lybaert, Timo Otonkoski, Conny Gysemans, Wei Wu, Esteban N. Gurzov

Exp ID	Age (Years)	Gender	BMI (kg/m^2)	Cause of death
#1	87	M	35,1	Trauma
#2	75	F	27,3	Vascular
#3	46	F	25,4	Anoxia

Supplementary Table S1. Pancreas organ donor characteristics for ER stress in dispersed human islets (Figure 5F).

Stage	Compound	Final concentration	Company
1 (3 days, change medium every day)	MCDB131 no Glutamine		Life Technologies, #10372-019
	GlutaMAX	2mM	Thermo Fisher, #35050
	NaHCO3	1.5g/l	Merck Millipore, #1063290500
	BSA fV	0.5%	Sigma, #A7030
	Glucose	10mM	Sigma, #G8769
	Activin A	100ng/ml	PeproTech, #120-14E
	CHIR	5µM (day 1), 0.5µM (day 2)	Axon Medchem, #1386
2 (3 days, change medium every day)	MCDB131 no Glutamine		Life Technologies, #10372-019
	GlutaMAX	2mM	Thermo Fisher, #35050
	NaHCO3	1.5g/l	Merck Millipore, #1063290500
	BSA fV	0.5%	Sigma, #A7030
	Glucose	10mM	Sigma, #G8769
	L-Ascorbic acid	0.25mM	Sigma, #A4554
	FGF-7	50ng/mL	PeproTech, #100-19
3 (2 days, change medium every day)	MCDB131 no Glutamine		Life Technologies, #10372-019
	GlutaMAX	2mM	Thermo Fisher, #35050
	NaHCO3	2.5g/l	Merck Millipore, #1063290500
	BSA fV	2%	Sigma, #A7030
	Glucose	10mM	Sigma, #G8769
	L-Ascorbic acid	0.25mM	Sigma, #A4554
	FGF-7	50ng/mL	PeproTech, #100-19
	SANT-1	0.25 µM	Sigma, #S4572
	Retinoic acid (RA)	1µM	Sigma, #R2625
	LDN-193189	100nM	Selleckchem, #S2618
	ITS-X	1:200	Thermo Fisher, #51500056
	TPB	200nM	Santa Cruz, #SC-204424
4 (4 days, change medium every day)	MCDB131 no Glutamine		Life Technologies, #10372-019
	GlutaMAX	2mM	Thermo Fisher, #35050
	NaHCO3	2.5g/l	Merck Millipore, #1063290500
	BSA fV	2%	Sigma, #A7030
	Glucose	10mM	Sigma, #G8769
	L-Ascorbic acid	0.25mM	Sigma, #A4554
	FGF-7	50 ng/mL	PeproTech, #100-19
	SANT-1	0.25µM	Sigma, #S4572
	Retinoic acid (RA)	0.1µM	Sigma, #R2625
	LDN-193189	200nM	Selleckchem, #S2618
	EGF	100ng/ml	StemCell Technologies, #78006
	Nicotinamide	10mM	Sigma, #N3376
	Activin A	10ng/ml	PeproTech, #120-14E
5 (4 days, change medium every day)	MCDB131 no Glutamine		Life Technologies, #10372-019
	GlutaMAX	2mM	Thermo Fisher, #35050
	NaHCO3	1.5g/l	Merck Millipore, #1063290500
	BSA fV	2%	Sigma, #A7030
	Glucose	20mM	Sigma, #G8769
	ITS-X	1:200	Thermo Fisher, #51500056
	Heparin	10µg/mL	StemCell Technologies, #07980
	Zinc Sulfate	10µM	Sigma, #Z0251
	Retinoic acid (RA)	0.05µM	Sigma, #R2625
	SANT-1	0.25µM	Sigma, #S4572
	LDN-193189	100nM	Selleckchem, #S2618
	GC-1	1µM	Tocris, #4554
	GSiXX	100nM	Merck Millipore, #565790
	ALK5inhII	10µM	ENZO, #ALX-270-445
	Betacellulin	20ng/ml	PeproTech, #100-50
	Penicillin - Streptomycin	100U/ml - 0.1mg/ml	Sigma, #P4333
	ROCK inhibitor Y-27632	10µM	StemCell Technologies, #72304
	Heparin	10ng/ml	StemCell Technologies, #07980
6 (7-8 days, change medium every second day)	MCDB131 no Glutamine		Life Technologies, #10372-019
	GlutaMAX	2mM	Thermo Fisher, #35050
	NaHCO3	1.5g/l	Merck Millipore, #1063290500
	BSA fV	2%	Sigma, #A7030
	Glucose	20mM	Sigma, #G8769
	ITS-X	1:200	Thermo Fisher, #51500056
	Heparin	10µg/mL	StemCell Technologies, #07980
	Zinc Sulfate	10µM	Sigma, #Z0251
	LDN-193189	100nM	Selleckchem, #S2618
	ALK5inhII	10µM	ENZO, #ALX-270-445
	GC-1	1µM	Tocris, #4554
	GSiXX	100nM	Merck Millipore, #565790
	Penicillin - Streptomycin	100U/ml - 0.1mg/ml	Sigma, #P4333
7 (8 days, change medium every second day)	MCDB131 no Glutamine		Life Technologies, #10372-019
	GlutaMAX	2mM	Thermo Fisher, #35050
	NaHCO3	1.5g/l	Merck Millipore, #1063290500
	BSA fV	2%	Sigma, #A7030
	Glucose	20mM	Sigma, #G8769
	ITS-X	1:200	Thermo Fisher, #51500056
	Heparin	10µg/mL	StemCell Technologies, #07980
	Zinc Sulfate	10µM	Sigma, #Z0251
	GC-1	1µM	Tocris, #4554
	Trolox	10µM	Sigma, #238813
	JNKi (SP600125)	20µM	Selleckchem, #SP600125
	RSV	75µM	Sigma, #R5010
	R428	2µM	Selleckchem, #S2841
	N-acetyl-cystein (NAC)	1mM	Sigma, #A9165
	Penicillin - Streptomycin	100U/ml - 0.1mg/ml	Sigma, #P4333

Supplementary Table S2. List of molecules used for stem cell differentiation into β-like cells.

Antibody	Company	Reference	Dilution
			Western blot
PTPN2	R&D Systems	MAB1930	1:300
PTPN2	Sigma-Aldrich	HPA015004	1:1000
pSTAT1 (Y701)	Cell Signaling	7649	1:1000
STAT1	Cell Signaling	14994	1:1000
STAT1	Cell Signaling	9176	1:1000
pSTAT3 (Y705)	Cell Signaling	9131	1:1000
STAT3	Cell Signaling	9139	1:1000
IκBα	Cell Signaling	9242	1:1000
BiP	Cell Signaling	3177	1:1000
ATF3	Santa Cruz Biotechnology	SC-188	1:500
ATF4	Cell Signaling	11815	1:1000
peIF2α	Cell Signaling	3597	1:1000
Cleaved caspase 3	Cell Signaling	9661	1:300
GAPDH	Trevigen	2275-PC-100	1:5000
α-tubulin	Sigma-Aldrich	T5168	1:5000
β-actin	Sigma-Aldrich	A1978	1:2000
Anti-Mouse IgG HRP	Dako	P0447	1:5000
Anti-Rabbit IgG HRP	Dako	P0448	1:5000
			Immunofluorescence
PTPN2	Sigma-Aldrich	HPA015004	1:100/1:250
GRP94	Thermo Fisher	MA3016	1:200
BiP/GRP78 Alexa fluor 488	Thermo Fisher	PA1-014A-A488	1:100
MANF	Sigma-Aldrich	ABN306	1:500
OCT4-A	Cell Signaling	2840	1:400
SOX17	R&D systems	AF1924	1:400
NKX6.1	BD Biosciences	563022	1:250
PDX1	R&D systems	AF2419	1:500
Insulin (cells)	Dako	IR002	1:500
Insulin (pancreas slides)	Dako	A0564	1:5000
Glucagon	Sigma	G2654	1:1000
OCT4	Santa Cruz Biotechnology	SC-9081	1:500
TRA-1-60	Thermo Fisher	MA1-023	1:250
SSEA4	Thermo Fisher	MA1-021-D488	1:250
Anti-Mouse-Alexa 488	Thermo Fisher	A21202	1:500/1:1000
Anti-Rabbit-Alexa 488	Thermo Fisher	A21206	1:500/1:1000
Anti-Rat-Alexa 488	Thermo Fisher	A11006	1:1000
Anti-Guinea pig-Alexa 488	Thermo Fisher	A11073	1:500/1:1000
Anti-Mouse-Alexa 555	Thermo Fisher	A32773	1:500/1:1000
Anti-Rabbit-Alexa 555	Thermo Fisher	A32794	1:500/1:1000
Anti-Guinea-Pig-Alexa 555	Thermo Fisher	A21435	1:1000
Anti-Goat-Alexa 555	Thermo Fisher	A32816	1:500
Anti-Guinea-Pig-Alexa 568	Thermo Fisher	A11075	1:500
Anti-Goat-Alexa 568	Thermo Fisher	A11057	1:500

Supplementary Table S3. List of antibodies used for Western blot and immunofluorescence analysis.

siRNA name	Company/catalogue number	Sequence (5' -> 3')
PTPN2 #1	Life Technologies-Ambion, 4390824	GGAGAUUCUAGUAUACAGA
PTPN2 #2	Life Technologies-Ambion, 4427038	GUACAGGACUUUCCUCUAA
PTPN2 #3	Qiagen, Hilden, Germany, SI02225895	CCGCTGTACTTGGAAATTCGA
PTPN2 #4	Qiagen, Hilden, Germany, SI02759239	CACAAAGGAGTTACATCTTAA
PTPN2 #5	Qiagen, Hilden, Germany, SI04898222	CAGGGTCCACTTCCTAACACA
PTPN2 #6	Qiagen, Hilden, Germany, SI04950400	TCCCATGACTATCCTCATAGA
STAT1	Life Technologies-Invitrogen, STAT1HSS110273	GGAUUGAAAGCAUCCUAGAACUCAU
STAT3	Qiagen, Hilden, Germany, SI02662338	CAGCCTCTCTGCAGAATTCAA

Supplementary Table S4. List of siRNAs for knockdown experiments.

Gene name	Primer sequences or catalogue number
PTPN2 (Human)	F: ATCGAGCGGGAGTTCGA R: TCTGGAAACTTGGCCACTC
PTPN2 (Mouse)	F: TCTGGAAACTTGGCCACTC R: ATCGAGCGGGAGTTCGA
CXCL9 (Human)	F: GAGGGCAAGAGCCACAGTAT R: GCCATCCTGCCCATAACA
CXCL10 (Human)	F: GTGGCATTCAAGGAGTACCTC R: GCCTTCGATTCTGGATTCAG
HLA-A (Human)	F: CAGGAGACACGGAATGTGAA R: TTATCTGGATGGTGTGAGAACC
STAT1(Human)	F: GACCCAATCCAGATGTCTATGA R: CCCGACTGAGCCTGATTA
STAT3(Human)	F: CTTTGAGACCGAGGTGTATCACC R: GGTCAGCATGTTGTACCACAGG
BiP (Human)	QT00096404 (Qiagen, Hilden, Germany)
CHOP (Human)	QT00082278 (Qiagen, Hilden, Germany)
ATF3 (Human)	F: GCTGTCACCACGTGCAGTAT R: TTTGTGTTAACGCTGGGAGA
ATF4 (Human)	F: GTCCTGTCCTCCACTCCAGA R: AGGGATCATGGCAACGTAAG
Insulin (Human)	F: CCAGCCGCAGCCTTTGTGA R: CCAGCTCCACCTGCCCCA
OCT4 (Human)	F: TTGGGCTCGAGAAGGATGTG R: TGCATAGTCGCTGCTTGATC
SOX2 (Human)	F: GCCCTGCAGTACAACTCCAT R: TGCCCTGCTGCGAGTAGG
NANOG(Human)	F: CTCAGCCTCCAGCAGATGC R: TAGATTTCATTCTCTGGTTCTGG
PTPN2 Exon ¾ (Human)	F: TCACAGTCGTGTTAAACTGCA R: CTGCTTTGGTCTTCTGCTGC
PPIG (Human)	F: TCTTGTCAATGGCCAACAGAG R: GCCCATCTAAATGAGGAGTTG
GAPDH (Human)	F: CAGCCTCAAGATCATCAGCA R: TGTGGTCATGAGTCCTTCCA
β-actin (Human)	F: CTGTACGCCAACACAGTGCT R: GCTCAGGAGGAGCAATGATC
β-actin (Mouse)	F: ACGGCCAGGTCATCACTATT R: GTTGGCATAGAGGTCTTTACG

Supplementary Table S5. List of probes used for qPCR. Real-time quantitative PCR was performed using the Biorad CFX96 machine (Biorad, Hercules, CA) and the SYBR green PCR Master Mix (Biorad). F: forward R: reverse.

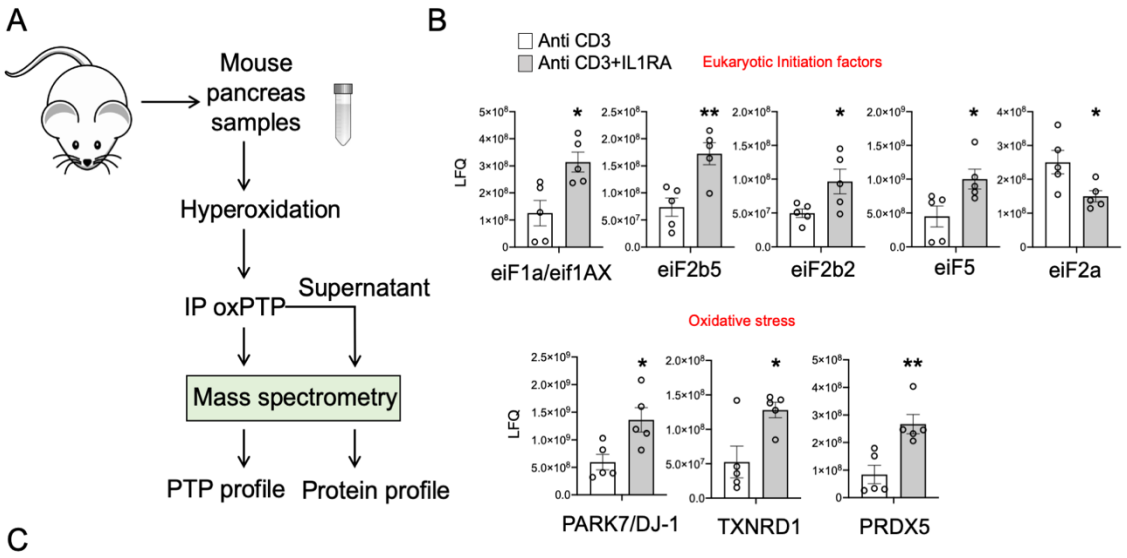

C

By summed spectra from 3 injection replicates

Uniprot Accession	Protein name	Gene names	Anti-CD3 #1	Anti-CD3 #2	Anti-CD3 #3	Anti-CD3 + IL1-RA #1	Anti-CD3 + IL-1RA #2	Anti-CD3 + IL1-RA #3	Anti-CD3 + IL-1RA #4	Anti-CD3 + IL-1RA #5	Peptide sequence 1	Peptide sequence 2
Q3TU63	Receptor-type tyrosine-protein phosphatase epsilon	Ptpre	0	0	0	0	0	2	1	2	TLNPSHAGPIVVHCSAGVGR	
A0A1W2P706	Receptor-type tyrosine-protein phosphatase kappa	Ptprk	0	2	4	2	3	2	4	6	LSNPPSAGPIVVHCSAGAGR	
Q3TS01	Receptor-type tyrosine-protein phosphatase beta	Ptprb	0	0	0	0	0	0	0	1	SPGAGPTVVHCSAGVGR	
Q3TT24	Receptor-type tyrosine-protein phosphatase F	Ptprf	0	0	1	0	0	0	0	0	EQFGQDGPITVHCSAGVGR	
Q3UND4	Receptor-type tyrosine-protein phosphatase gamma	Ptprg	0	1	1	0	0	0	0	1	MPDMGPVLVHCSAGVGR	
Q8C6Q7	Receptor-type tyrosine-protein phosphatase C	Ptprc	0	0	0	0	0	0	0	6	VNAFSNFFSGPIVVHCSAGVGR	
Q91V35	Receptor-type tyrosine-protein phosphatase alpha	Ptpra	0	0	0	1	1	0	5	9	ACNPQYAGAIVVHCSAGVGR	QQQQSGNHPITVHCSAGAGR
Q3V3S2	Receptor-type tyrosine-protein phosphatase mu	Ptprm	0	2	2	1	0	0	1	6	SPPNAGPLVVHCSAGAGR	
Q3UB72	Tyrosine-protein phosphatase non-receptor type 6	Ptpn6	2	4	2	3	4	3	4	6	QESLPHAGPIIVHCSAGIGR	
P35235	Tyrosine-protein phosphatase non-receptor type 11	Ptpn11	6	6	8	10	10	9	8	9	QESIVDAGPVVVHCSAGIGR	
Q3T9Y9	Tyrosine-protein phosphatase non-receptor type 1	Ptpn1	2	2	3	4	3	3	4	3	ESGSLSLEHGPIVVHCSAGIGR	
P35831	Tyrosine-protein phosphatase non-receptor type 12	Ptpn12	0	0	0	0	0	0	1	2	YQEHEDVPICIHCSAGCGR	
Q9WU22	Tyrosine-protein phosphatase non-receptor type 4	Ptpn4	0	0	3	0	0	0	0	1	EEPIIVHCSAGIGR	
Q3TPD6	Tyrosine-protein phosphatase non-receptor type 13	Ptpn13	3	3	4	3	3	3	3	5	SGPVITHCSAGIGR	
A2ALK8	Tyrosine-protein phosphatase non-receptor type 3	Ptpn3	1	2	1	2	0	1	1	0	VDGEPALVHCSAGIGR	
D3Z6W2	Tyrosine-protein phosphatase non-receptor type 2	Ptpn2	0	0	0	4	3	3	5	2	ESGCLTPDHGPAVIHCSAGIGR	
Q2M4G8	Tyrosine-protein phosphatase non-receptor type 9	Ptpn9	0	0	0	0	0	0	0	1	GQCPEPPIVVHCSAGIGR	
		PSM total	14	22	29	30	27	26	37	60		

Supplementary Figure S1. Combined treatment of anti-CD3 and IL-1 receptor antagonist (IL-1RA) cured NOD mice. (A) Protocol scheme to study the global proteomics and PTP profile from murine pancreas samples. **(B)** Protein profile of pancreata was examined by mass spectrometry. Protein expression of eukaryotic initiator factors and oxidative stress-related proteins is shown. LFQ: label-free quantification. n=5. **(C)** Spectral counts of oxPTP peptides in anti-CD3 + IL-1RA-treated or anti-CD3 control NOD mice. PSM: peptide-spectrum match. *p<0.05, **p<0.01.

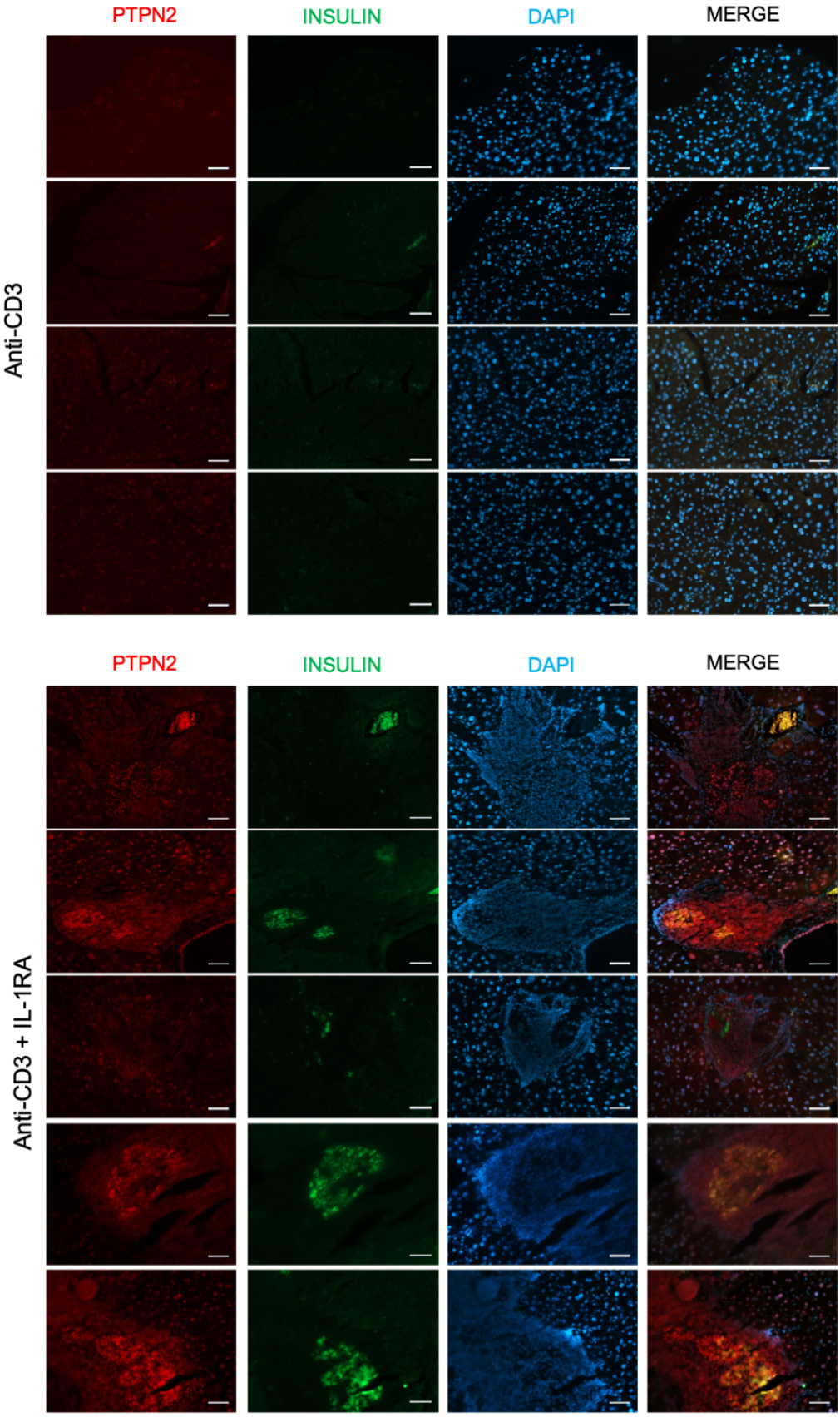

Supplementary Figure S2. Increased PTPN2 expression in mice with combined treatment of anti-CD3 + IL-1 receptor antagonist (IL-1RA). Immunofluorescence analysis of insulin and PTPN2 in pancreas sections derived from mice with anti-CD3 antibody + IL-1RA or controls. The nuclei were visualized with DAPI. Scale bar: 50µm.

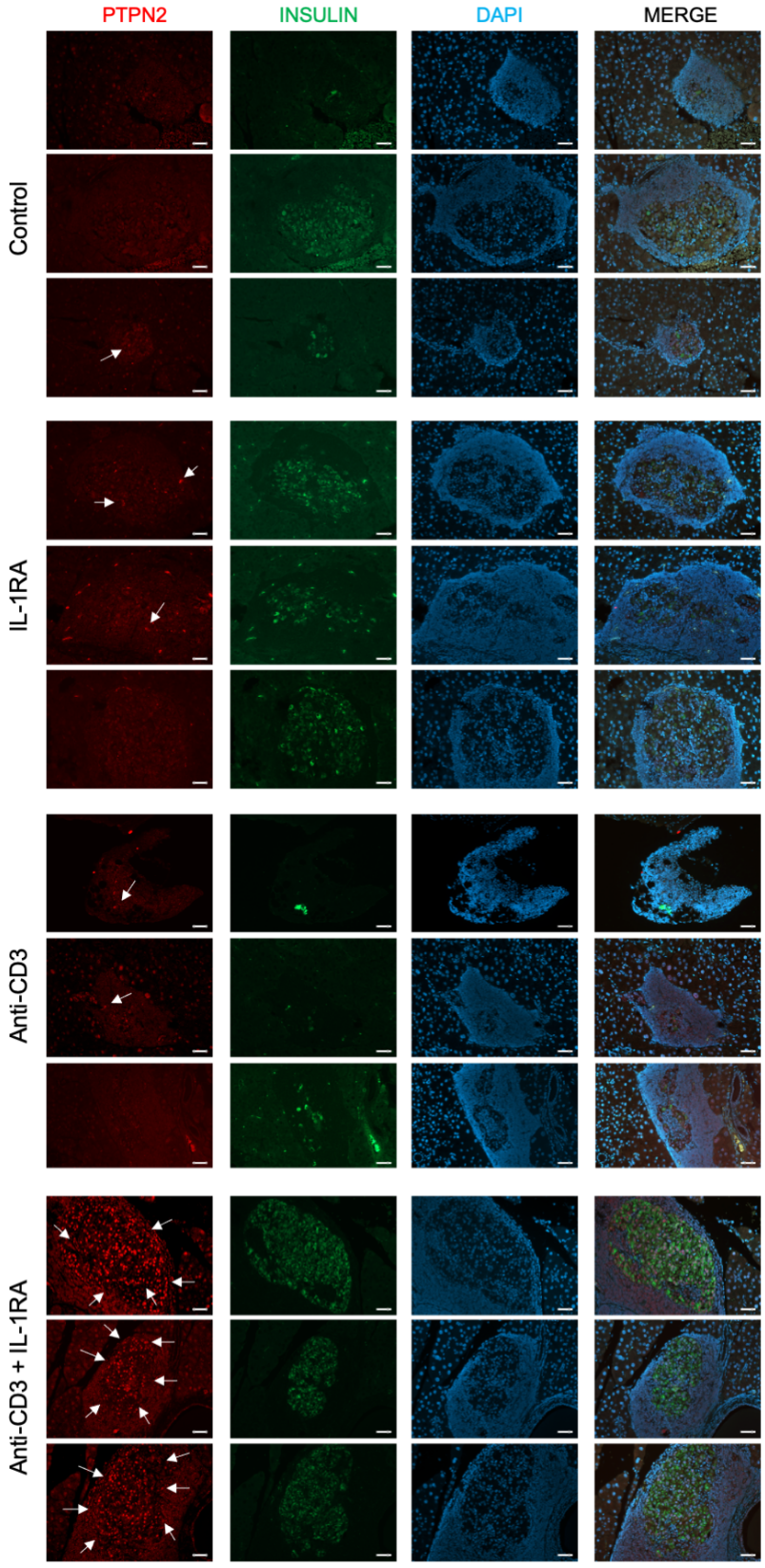

Supplementary Figure S3. High PTPN2 expression in islets from mice with anti-CD3 + IL-1 receptor antagonist (IL-1RA). Immunofluorescence analysis of insulin and PTPN2 in pancreas sections derived from mice without treatment (control), IL-1RA, anti-CD3 antibody, or anti-CD3 antibody + IL-1RA. The nuclei were visualized with DAPI. PTPN2 expression in insulin positive cells is shown (white arrows). Scale bar: 50μm.

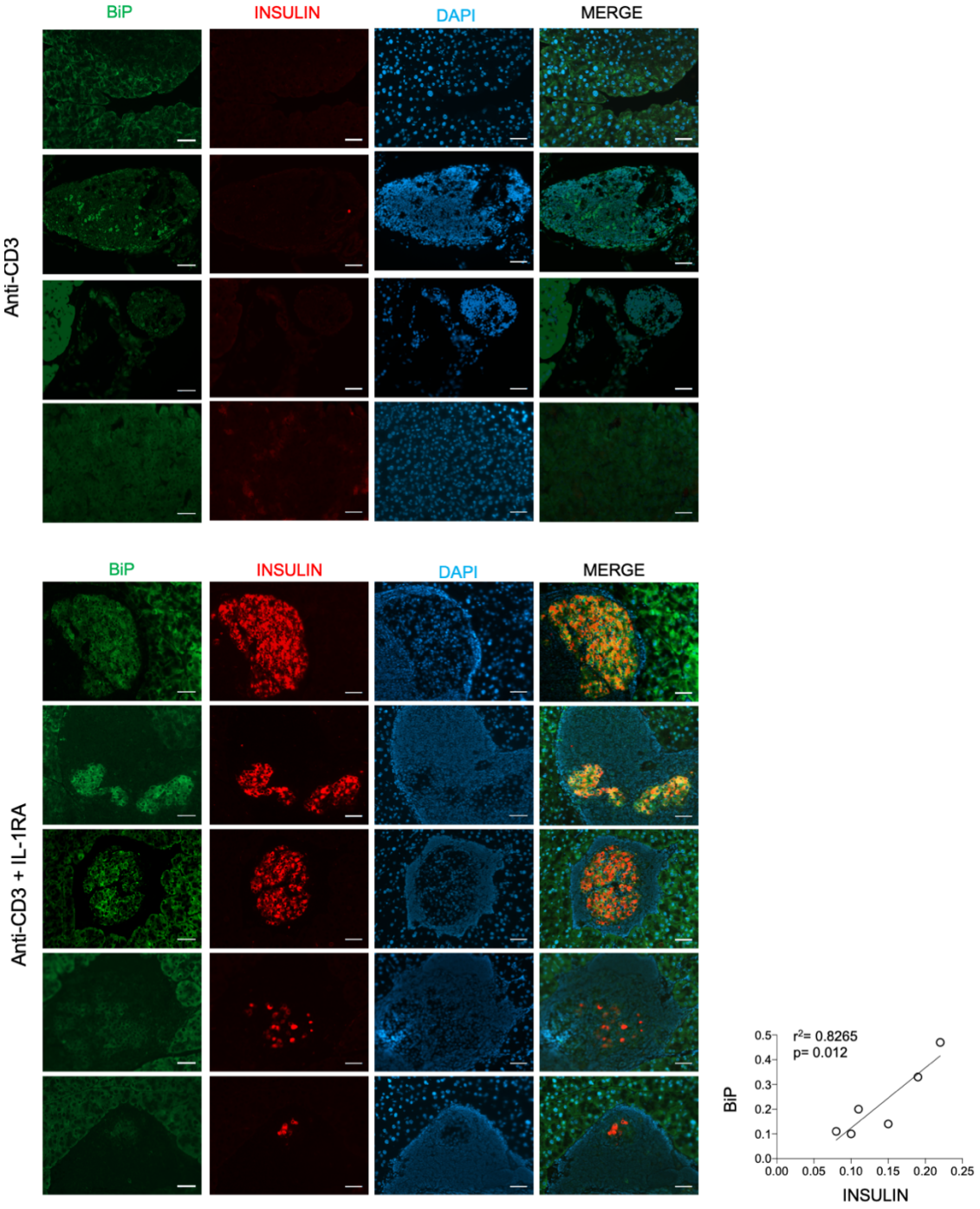

Supplementary Figure S4. Increased BiP expression in mice with combined treatment of anti-CD3 + IL-1 receptor antagonist (IL-1RA). Immunofluorescence analysis of insulin and ER stress response-related protein BiP in pancreas sections derived from mice with anti-CD3 + IL-1RA or controls. The nuclei were visualized with DAPI. Scale bar: 50µm. Insulin and GRP94 correlation in pancreatic islets from anti-CD3 + IL-1RA treatment is shown.

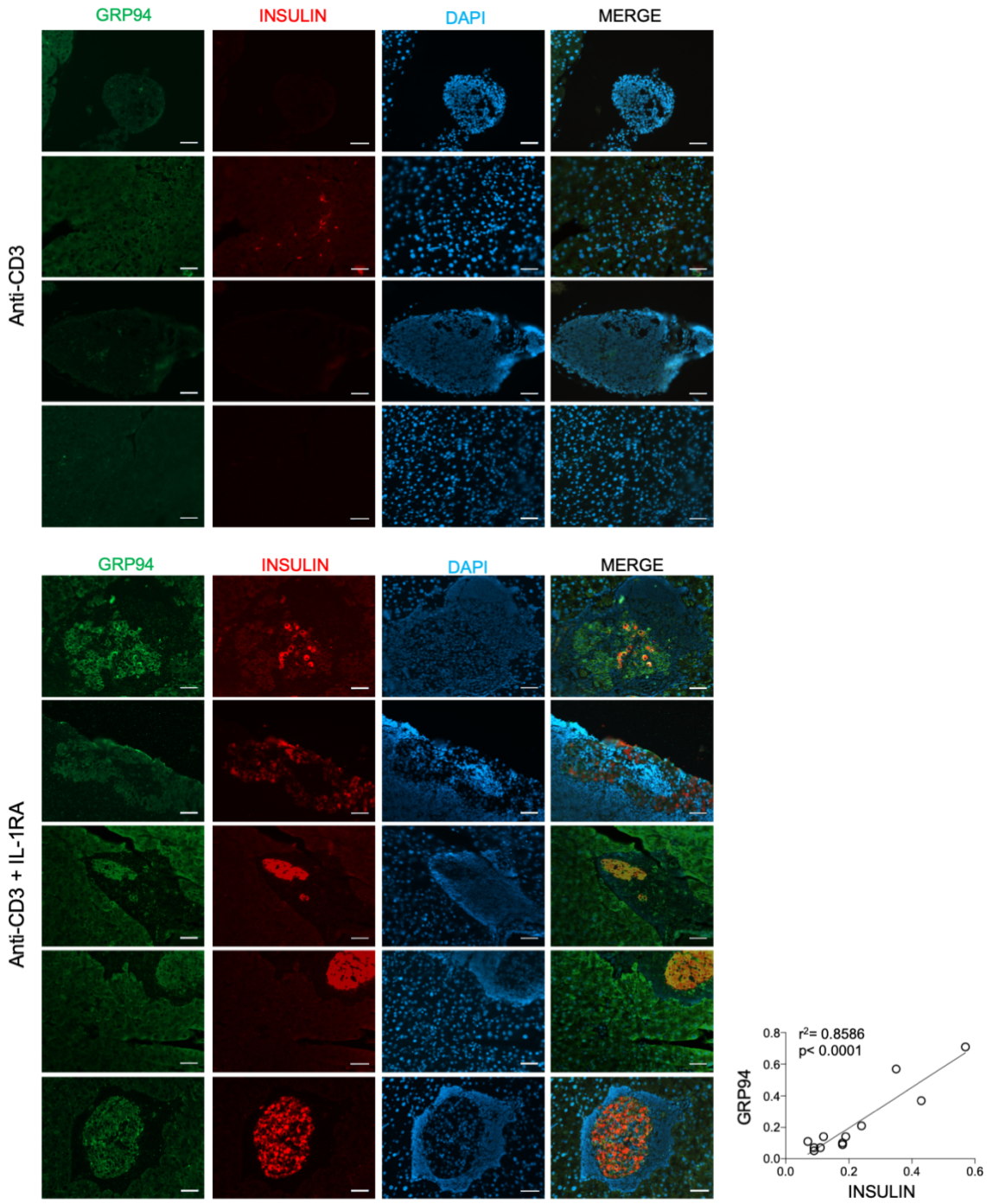

Supplementary Figure S5. Increased GRP94 expression in mice with combined treatment of anti-CD3 + IL-1 receptor antagonist (IL-1RA). Immunofluorescence analysis of insulin and ER stress response-related protein GRP94 in pancreas sections derived from mice with anti-CD3 + IL-1RA or controls. The nuclei were visualized with DAPI. Scale bar: 50µm. Insulin and GRP94 correlation in pancreatic islets from anti-CD3 + IL-1RA treatment is shown.

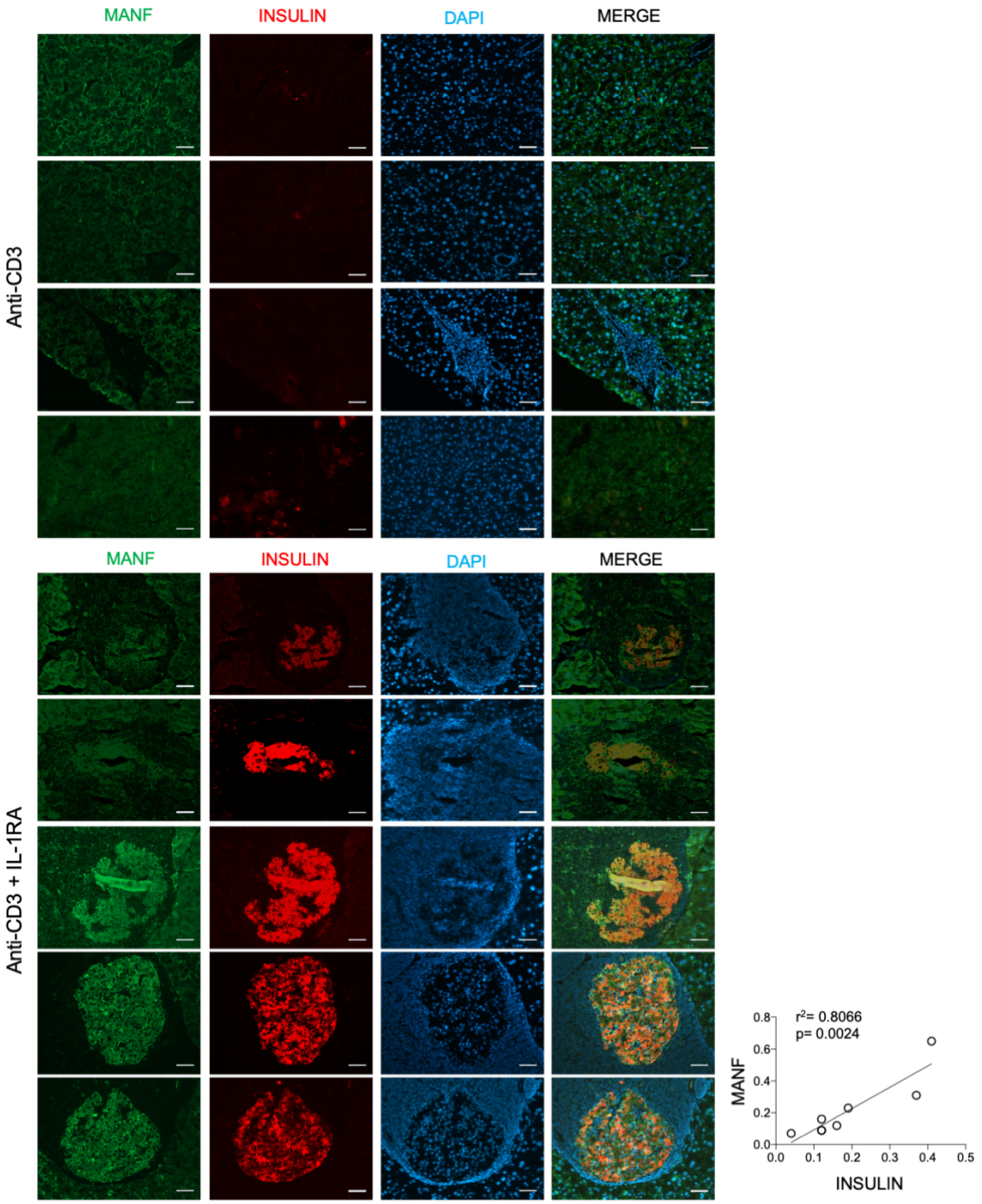

Supplementary Figure S6. Increased MANF expression in mice with combined treatment of anti-CD3 + IL-1 receptor antagonist (IL1RA). Immunofluorescence analysis of insulin and ER stress response-related protein MANF in pancreas sections derived from mice with anti-CD3 + IL-1RA or controls. The nuclei were visualized with DAPI. Scale bar: 50µm. Insulin and MANF correlation in pancreatic islets from anti-CD3 + IL-1RA treatment is shown.

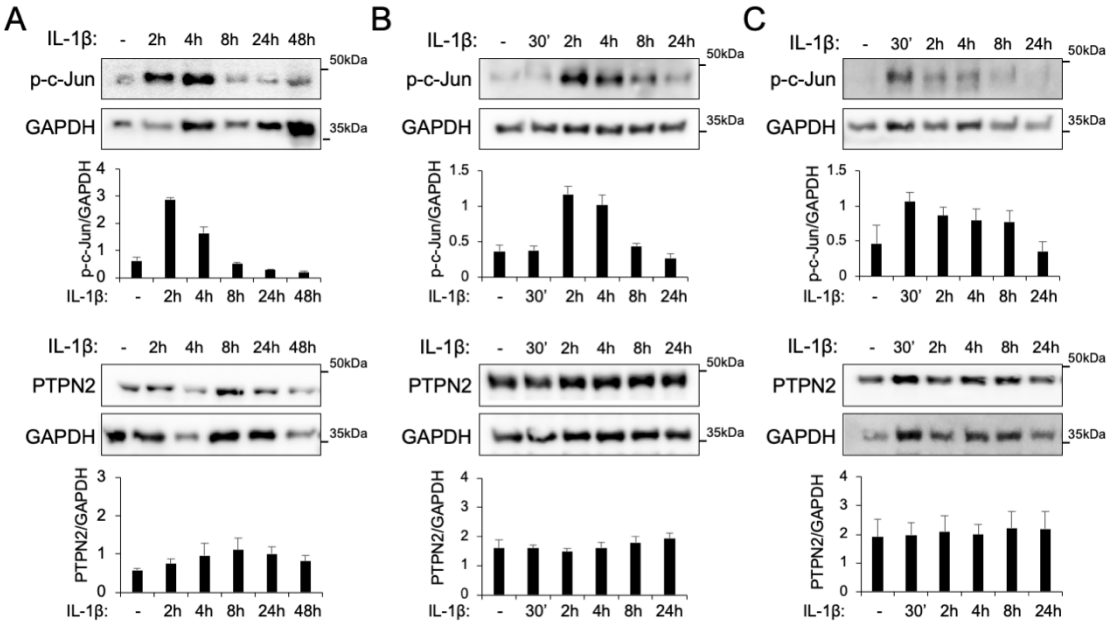

Supplementary Figure S7. IL-1β does not modulate PTPN2 in isles/β-cells. (A) C57BL/6 mouse islets were isolated and treated with IL-1β (50U/ml) as indicated. p-c-Jun (activated by IL-1β), PTPN2 and GAPDH were assessed by Western blot. n=2. **(B)** EndoC-βH1 cells were treated with IL-1β (50U/ml) as indicated. p-c-Jun (activated by IL-1β), PTPN2 and GAPDH were assessed by Western blot. n=4. **(C)** H1-differentiated β-like cells were treated with IL-1β (50U/ml) as indicated. p-c-Jun (activated by IL-1β), PTPN2 and GAPDH were assessed by Western blot. n=3.

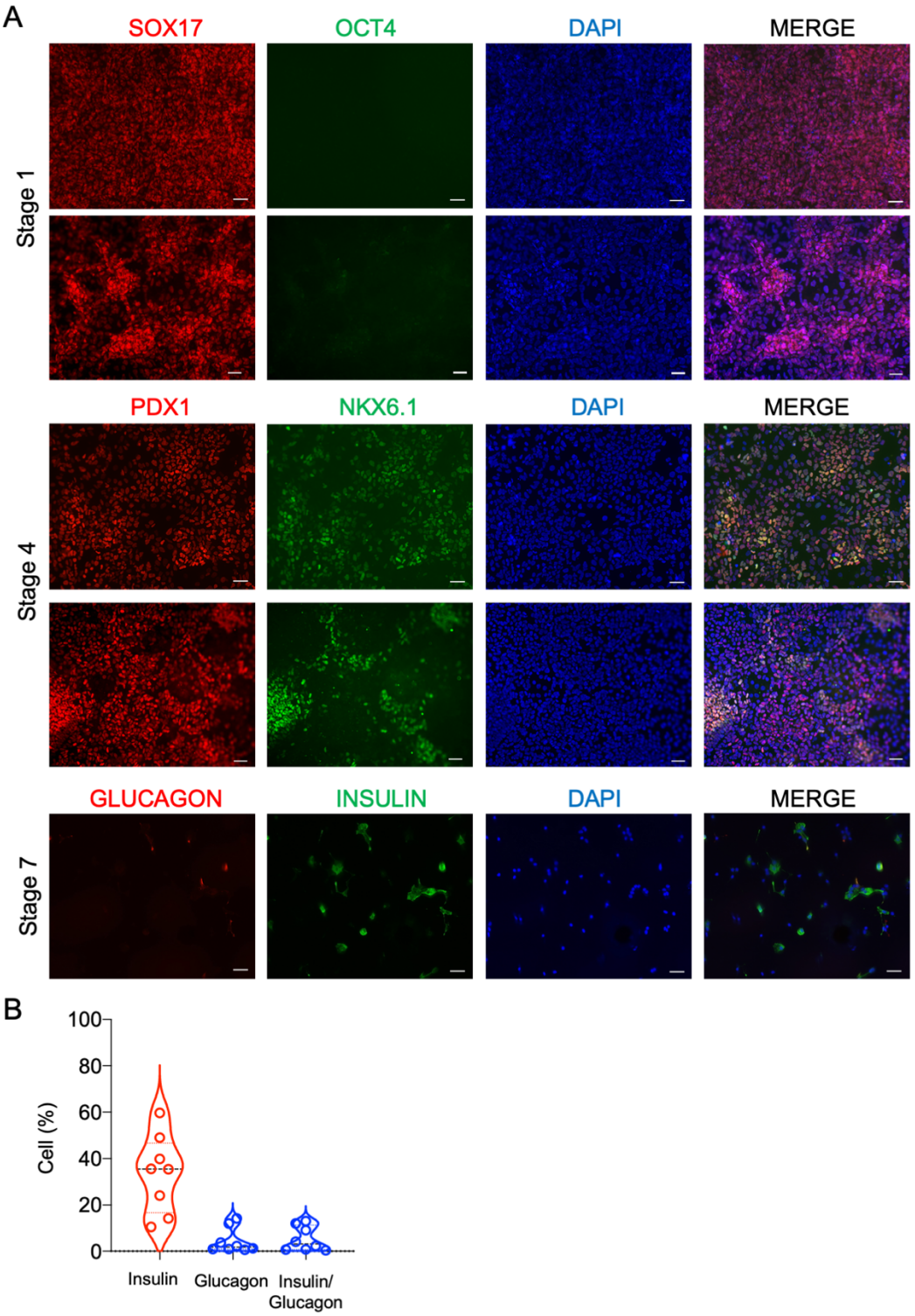

Supplementary Figure S8. Characterisation of stem cell differentiation. (A) Immunofluorescence staining of Hel46.11 hiPSC differentiation markers in the different stages as indicated. 2 independent differentiations are represented. **(B)** Percentage of insulin, glucagon and insulin/glucagon double-positive cells by immunofluorescence in insulin-producing Hel46.11 and H1 differentiated cells. The results are expressed as percentage of total cell number. n=8.

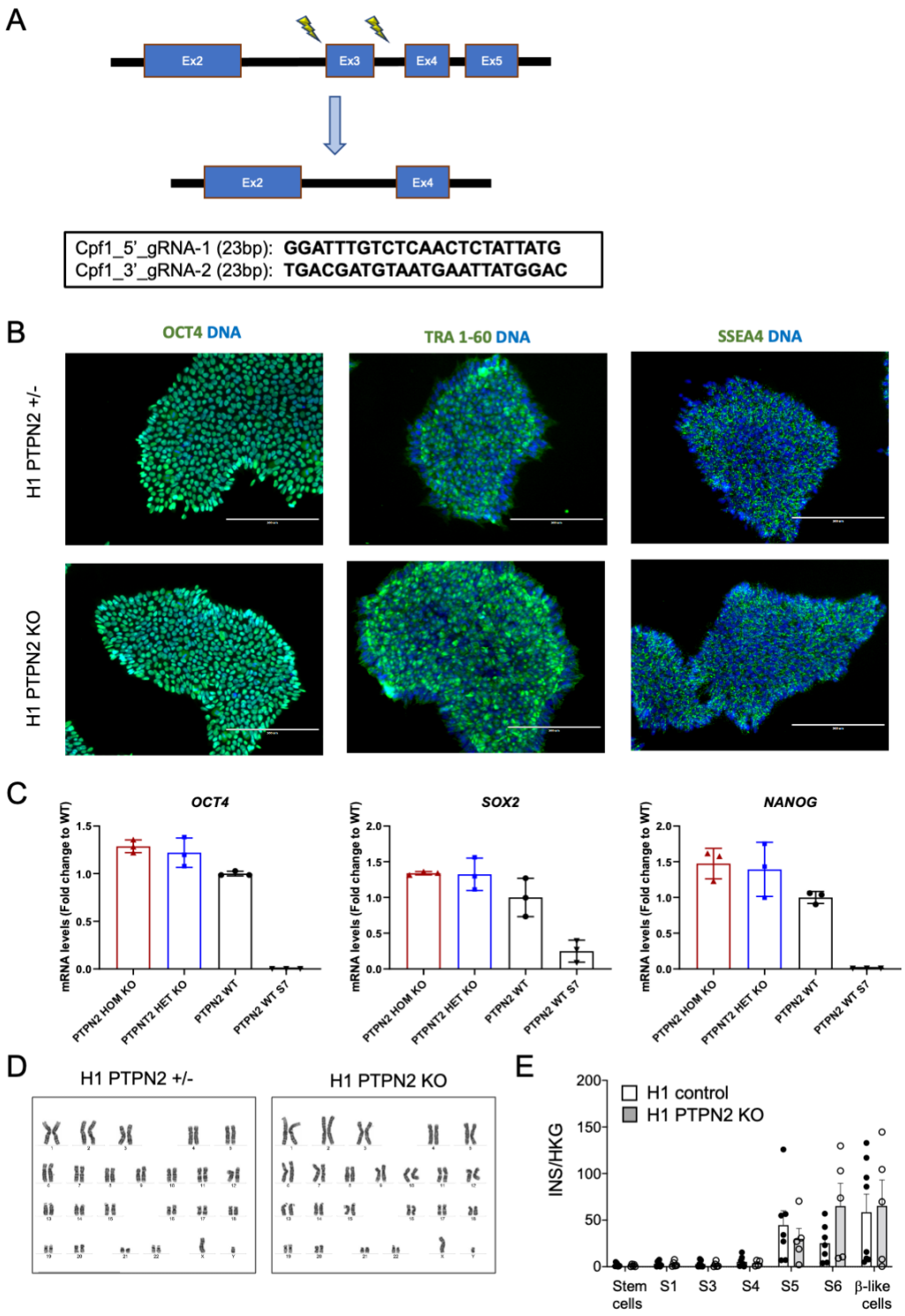

Supplementary Figure S9. Characterization of H1 cell lines with *PTPN2* gene editing using CRISPR/Cpf1. (A) Scheme of *PTPN2* exon 3 deletion. **(B)** Immunofluorescence staining of pluripotency markers (OCT4, TRA1-60 and SSEA4) in undifferentiated H1 cells. Scale bar: 200µm. **(C)** OCT4, SOX2 and NANOG mRNA expression assessed by real-time PCR in undifferentiated H1 cell lines and the stage 7 (S7) of H1 wild-type cell line. Results were normalised with PPIG as internal housekeeping control gene. n=3. **(D)** Karyotype of H1 wild-type and H1 homozygous knockout. **(E)** Insulin mRNA expression assessed by real-time PCR during the 7 stages of H1 cells differentiation into β-like cells. Results were normalized with mean of GAPDH and β-actin as internal housekeeping genes. n=5-8.

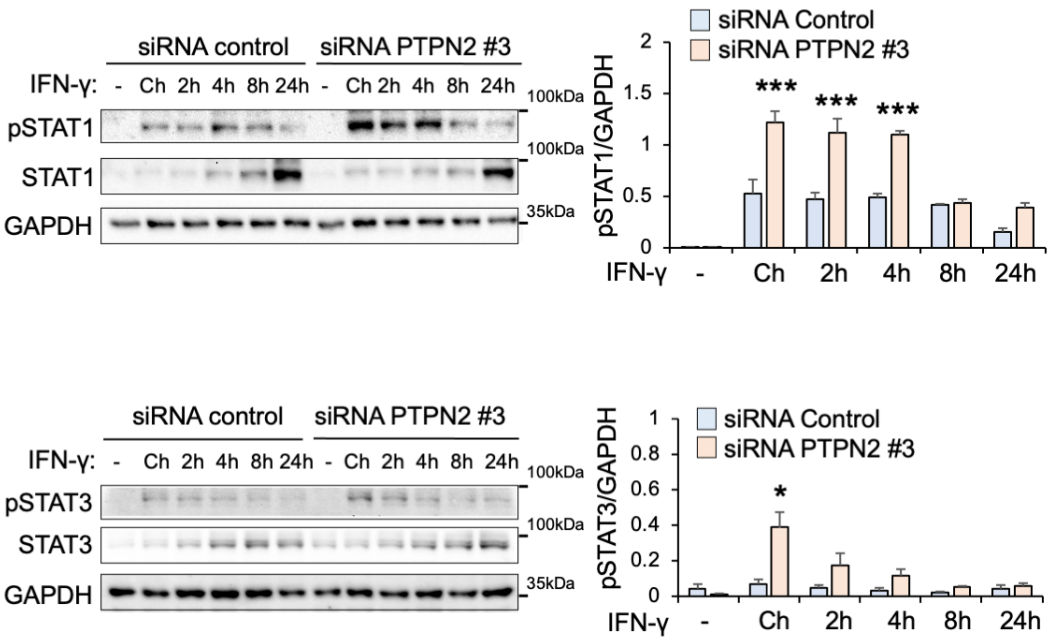

Supplementary Figure S10. PTPN2 regulates STAT1 and STAT3 phosphorylation in IFN-γ-treated β-cells. Transfected EndoC-βH1 cells with control or PTPN2 (#3) siRNA were cultured with the pro-inflammatory cytokine IFN-γ for 1h in a pulse-chase experiment. Western blot for pSTAT1, total STAT1, pSTAT3, total STAT3 and GAPDH was performed. Error bars represent ± SEM. N=4. *p<0.05, ***p<0.001.

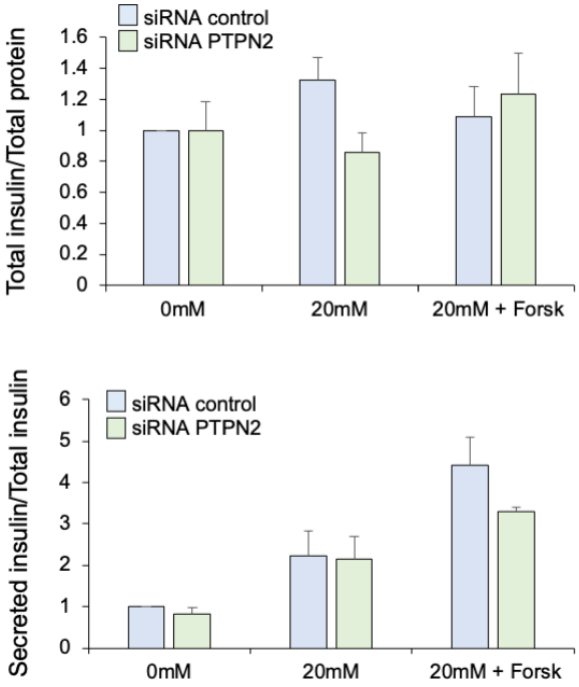

Supplementary Figure S11. PTPN2 deficiency does not affect glucose-induced insulin secretion in EndoC-βH1 cells. Total and secreted insulin analysis between siRNA PTPN2 or control transfected EndoC-βH1 cells without glucose, exposed to high glucose (20mM) or high glucose and forskolin (10µM, Sigma-Aldrich). Insulin was measure with an ELISA kit (Mercodia, NC, USA)**.** n=5.

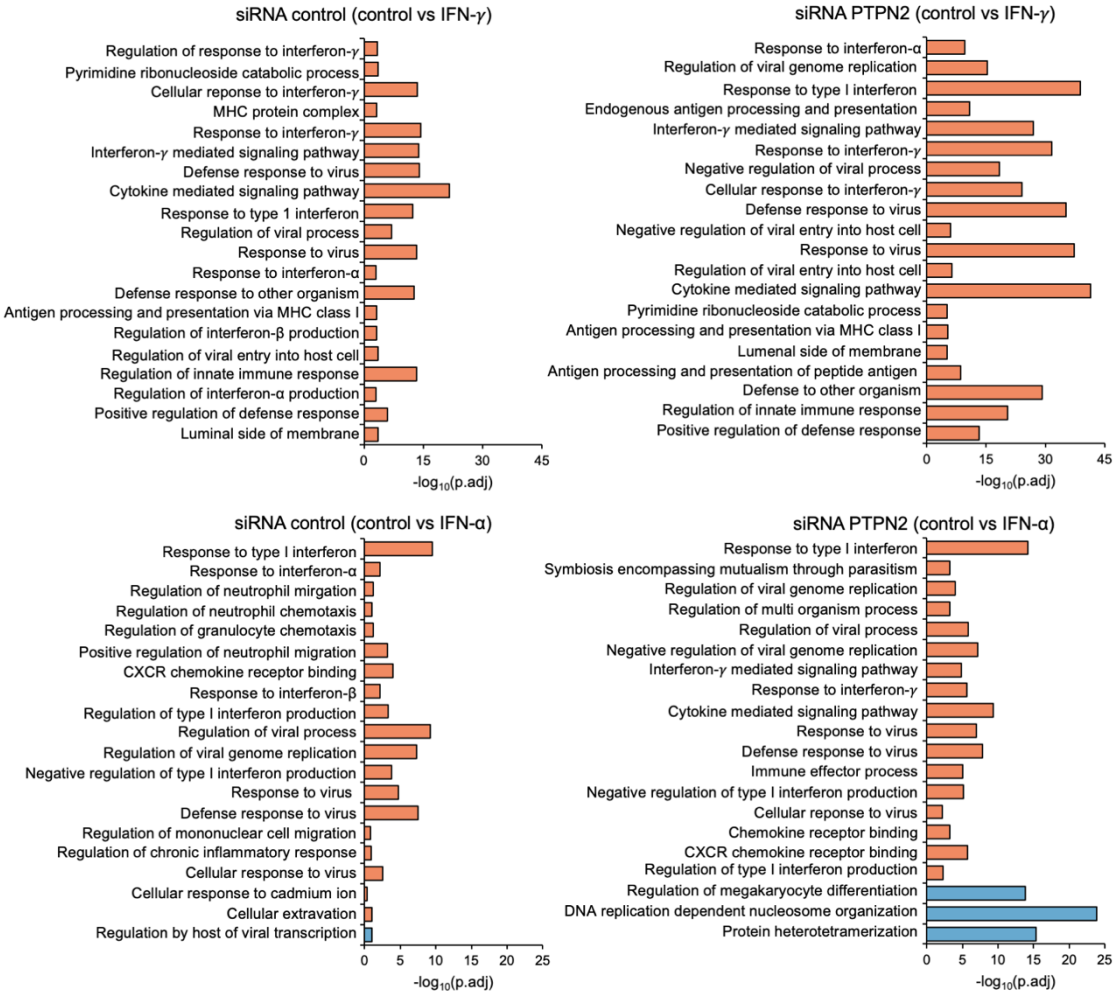

Supplementary Figure S12. PTPN2 regulates immune response pathways after cytokine treatment in β-cells. Pathway enrichment analysis of the comparison between siRNA PTPN2 or control transfected EndoC-βH1 cells and treated with IFN-γ or IFN-α. The length of the bars is proportional to the level of significant change, expressed by the negative logarithm of the adjusted p-value. Orange upregulated and blue downregulated pathways with $p < 0.05$ are shown**.**

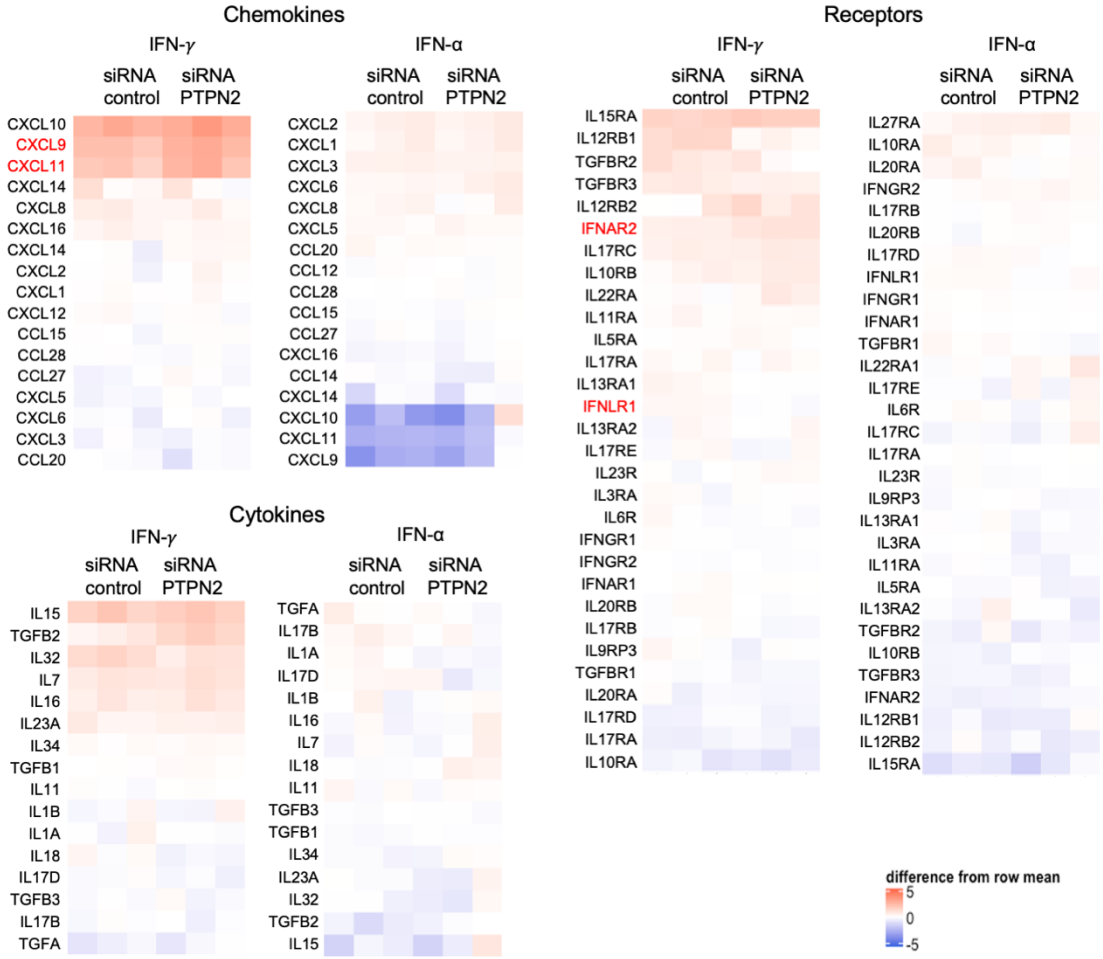

Supplementary Figure S13. Chemokines, cytokines and receptor expression in interferon-treated PTPN2 deficiency β-cells. Heatmap analysis of siRNA PTPN2 or control transfected EndoC-βH1 cells obtained by RNA-Seq. The counts are scaled to the difference of the row mean. Gene expression is considered significant upon an FDR<0.05 (showed in red). n=3.

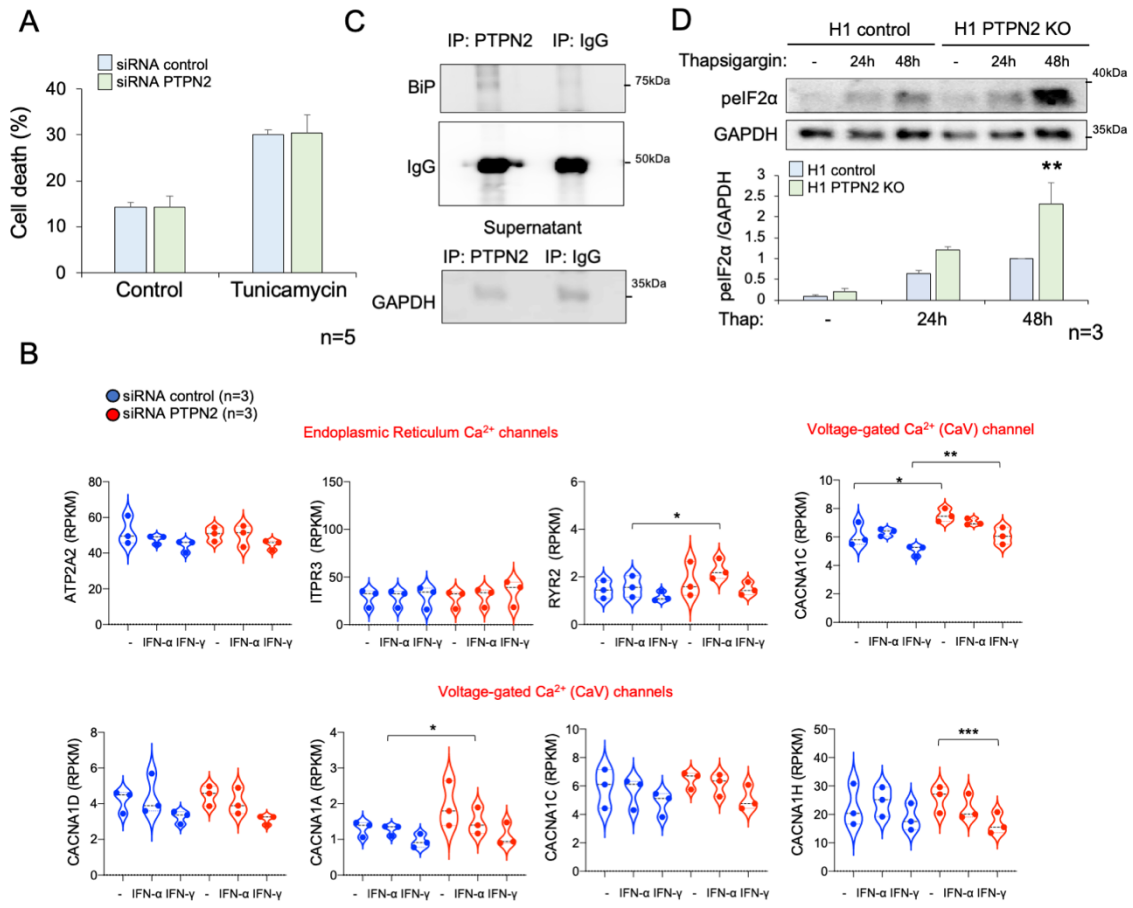

Supplementary Figure S14. The role of PTPN2 deficiency in β-cell death and Ca^{2+} channel expression. (A) Transfected cells with PTPN2 or control siRNAs were cultured with tunicamycin for 48h. β-cell apoptosis was evaluated by Hoechst 33342/propidium iodide staining. n=5. **(B)** Gene counts obtained by RNA-Seq were normalised to reads per kilobase million (RPKM) using Rstudio. n=3. **(C)** PTPN2 and control (IgG) immunoprecipitation of EndoC-βH1 cells transduced with AdPTPN2 48kDa. BiP binding was detected by Western blot analysis in the pull down. GAPDH levels in the supernatant is used as sample loading. The result is representative of 2 independent experiments. **(D)** Dispersed H1-derived β-like cells were cultured with thapsigargin for 24 or 48h as indicated. Protein expression of ER stress marker peIF2α was examined by Western blot. n=3. *p<0.05, **p<0.01, ***p<0.001.

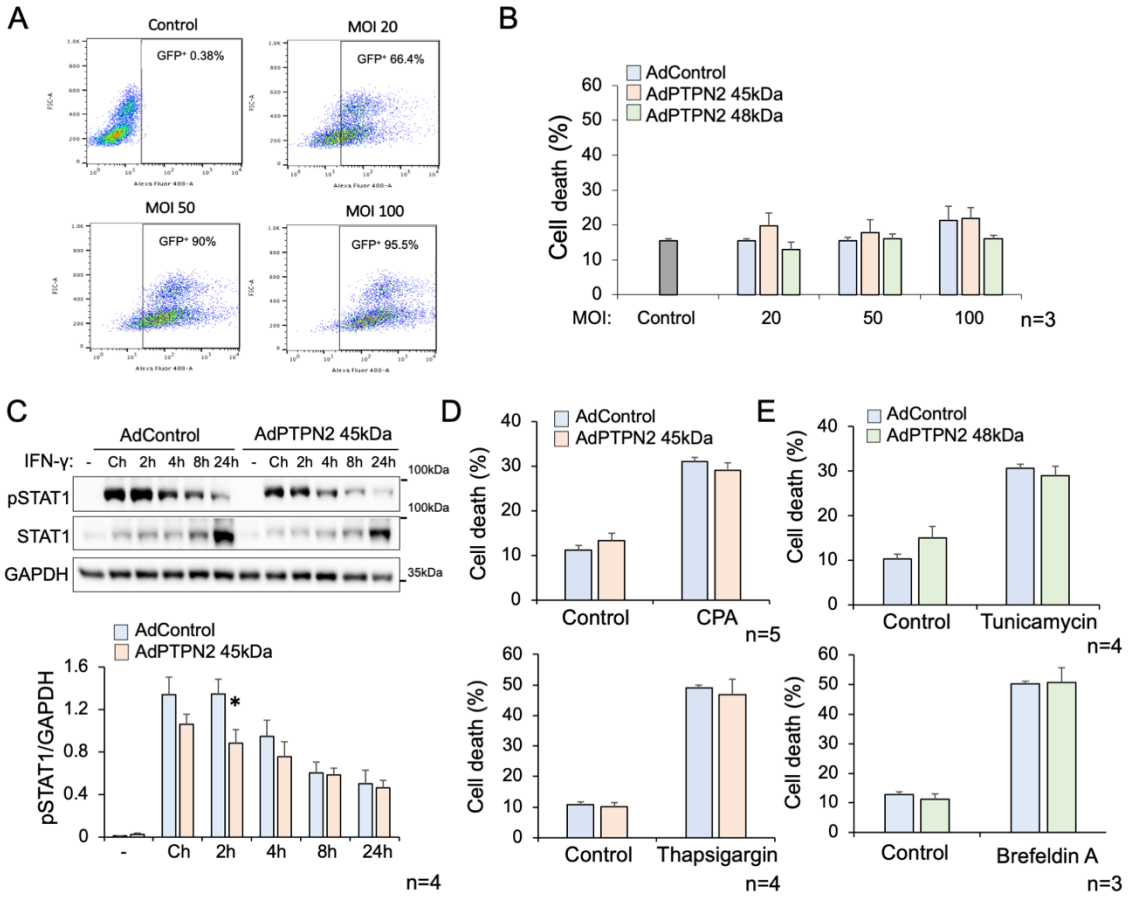

Supplementary Figure S15. Characterization of ER stress modulation by different PTPN2 isoforms. (A-B) EndoC-βH1 cells were transduced with AdControl, AdPTPN2 45kDa or AdPTPN2 48kDa. **(A)** Transduction efficiency counting GFP positive cells was measured by flow cytometry. **(B)** β-cell apoptosis was evaluated by Zombie Aqua™ staining and flow cytometry. n=3. **(C)** Transduced cells with AdPTPN2 45kDa or AdControl were cultured with the pro-inflammatory cytokine IFN-γ for 1h in a pulse-chase experiment. Western blot for pSTAT1, total STAT1. n=4. **(D)** Transduced cells with AdPTPN2 45kDa or AdControl were cultured either with CPA or with thapsigargin for 48h. β-cell apoptosis was evaluated by Hoechst 33342/propidium iodide staining. n=4-5. (**E**) Transduced cells with AdPTPN2 48kDa or AdControl were cultured either with tunicamycin for 48h or with brefeldin A for 24h. β-cell death was evaluated by Hoechst 33342/propidium iodide staining. n=3-4. *p<0.05.

American Diabetes Association. diabetes

Checklist for Reporting Human Islet Preparations Used in Research

Adapted from Hart NJ, Powers AC (2018) Progress, challenges, and suggestions for using human islets to understand islet biology and human diabetes. Diabetologia https://doi.org/10.1007/s00125-018-4772-2.

Manuscript DOI: https://doi.org/10.2337/db21-0443

Title: PTPN2 regulates the interferon signalling and endoplasmic reticulum stress response in pancreatic β-cells in autoimmune diabetes

Author list: Bernat Elvira, Valerie Vandenbempt, Julia Bauzá-Martinez, Raphaël Crutzen, Javier Negueruela, Hazem Ibrahim, Matthew L. Winder, Beata Vekeriotaite, Pieter-Jan Martens, Sumeet Pal Singh, Fernando Rossello, Pascale Lybaert, Timo Otonkoski, Conny Gysemans, Wei Wu, Esteban N. Gurzov

Corresponding author: Esteban N. Gurzov **Email address:** esteban.gurzov@ulb.be

Islet preparation	**1**	**2**	**3**	**4**	**5**	**6**	**7**	**8[a]**
MANDATORY INFORMATION								
Unique identifier	28-4-19	28-9-19	3-2-20					
Donor age (years)	87	75	46					
Donor sex (M/F)	M	F	F					

Donor BMI (kg/m^2)	35.1	27.3	25.4					
Donor HbA_{1c} or other measure of blood glucose control	Normal	Normal	Normal					
Origin/source of islets[b]	Prof Piero Marchetti	Prof Piero Marchetti	Prof Piero Marchetti					
Islet isolation centre	Pancreatic Islet Laboratory in Pisa-Italy	Pancreatic Islet Laboratory in Pisa-Italy	Pancreatic Islet Laboratory in Pisa-Italy					
Donor history of diabetes? Yes/No	No	No	No					
If Yes, complete the next two lines if this information is available								
Diabetes duration (years)								
Glucose-lowering therapy at time of death[c]								

RECOMMENDED INFORMATION								
Donor cause of death	Trauma	Vascular	Anoxia					
Warm ischaemia time (h)								

Cold ischaemia time (h)								
Estimated purity (%)	75	22	31					
Estimated viability (%)								
Total culture time (h)[d]	120	120	96					
Glucose-stimulated insulin secretion or other functional measurement[e]								
Handpicked to purity? Yes/No	Yes	Yes	Yes					
Additional notes								

[a]If you have used more than eight islet preparations, please complete additional forms as necessary
[b]For example, IIDP, ECIT, Alberta IsletCore
[c]Please specify the therapy/therapies
[d]Time of islet culture at the isolation centre, during shipment and at the receiving laboratory
[e]Please specify the test and the results